2007:30

LICENTIATE THESIS

Homogenization of Reynolds Equations

Emmanuel Kwame Essel

Luleå University of Technology
Department of Mathematics

2007:30 | ISSN: 1402-1757 | ISRN: LTU-LIC -- 07/30 -- SE

Homogenization of Reynolds Equations

by

Emmanuel Kwame Essel

Department of Mathematics
Luleå University of Technology
971 87 Luleå, Sweden

June 2007

Examiner
Professor Lars-Erik Persson,
Luleå University of Technology, Sweden

Published 2007
Printed in Sweden by University Printing Office, Luleå

To my wife and children

Abstract

This Licentiate thesis is focussed on some new questions in homogenization theory, which have been motivated by some concrete problems in tribology. From the mathematical point of view these questions are equipped with scales of Reynolds equations with rapidly oscillating coefficients. In particular, in this Licentiate thesis we derive the corresponding homogenized (averaged) equation. We consider the Reynolds equations in both the stationary and unstationary forms to analyze the effect of surface roughness on the hydrodynamic performance of bearings when a lubricant is flowing through it.

In Chapter 1 we describe the possible types of surfaces a bearing can take. Out of these we select two types and derive the appropriate Reynolds equations needed for their analysis.

Chapter 2 is devoted to the derivation of the homogenized equations associated with the stationary forms of the compressible and incompressible Reynolds equations. We derive these homogenized equations by using the multiple scales expansion technique.

In Chapter 3 the homogenized equations for the unstationary forms of the Reynolds equations are considered and some numerical results based on the homogenized equations are presented.

In Chapter 4 we consider the equivalent minimization problem for the unstationary Reynolds equation and use it to derive a homogenized minimization problem. Finally, we obtain both the lower and upper bounds for the derived homogenized problem.

Preface

This Licentiate thesis is written as a monograph. A brief description of the chapters are outlined in the abstract.

In particular the author's contributions in the following papers are included in this Licentiate thesis:

- A. Almqvist, E. K. Essel, L.-E. Persson and P. Wall, *Homogenization of the unstationary incompressible Reynolds equation*, Tribol. Int. (in press),(18 pages), 2007.

- A. Almqvist, E. K. Essel, J. Fabricius and P. Wall, *Bounds for the unstationary incompressible Reynolds equation,* Research Report (2007), Department of Mathematics, Luleå University of Technology, Sweden, submitted, (17 pages).

  Also the following paper has influenced the ideas in my studies, but the results are not included in this Licentiate thesis:

- E. K. Essel, *Homogenization of the Stationary Compressible Reynolds Equation by Two-scale Convergence (Constant Bulk Modulus Case),* Research Report **3** (2007), Department of Mathematics, Luleå University of Technology, Sweden, (16 pages).

Acknowledgements

I wish to express my profound gratitude to my main supervisor, Professor Lars-Erik Persson, for introducing me into this area of research. I have benefited immensely from his wealth of experience, constant encouragement, patience, pieces of advice and understanding which together has enhanced my research work.

I am also indebted to my co-supervisor Professor Peter Wall for his useful discussions, patience, support and willingness to assist me any time I called on him. For this I am very grateful.

My sincere thanks also go to my second co-supervisor Dr. Andreas Almqvist of the Department of Machine elements, Andreas Nilsson of the Computer Science department and my fellow Ph.D. student John Fabricius for sharing constructive ideas and maintaining a very good working relationship with me.

I wish to thank the Government of Ghana, the authorities of the University of Cape Coast, Cape Coast, Ghana, for being my main financial sponsors and the International Science Programme (I.S.P.), Uppsala, Sweden for their financial support. I am also very grateful to Professor F. K. A. Allotey, President of Institute of Mathematical Sciences, Accra, Ghana and Dr. Leif Abrahamson (I.S.P) for their immense support.

I would also like to thank the staff of the Department of Mathematics at Luleå University of Technology for putting at my disposal the necessary facilities needed for my work. Their marvelous hospitality and support has made my stay here a memorable one.

Finally, I wish to thank my wife, Mrs. Belinda G. Essel, and my children for their unflinching support, love and constant prayer.

Luleå, June 2007
Emmanuel Kwame Essel

Contents

Chapter 1

Introduction

1.1 Reynolds type equations

Reynolds type equations are applicable in the field of Tribology. Tribology is a multidisciplinary field, which deals with the science, practice and technology of lubrication, wear prevention and friction control in machines. This enable lubrication engineers to minimize cost of moving parts. In this way machinery can be made more efficient, more reliable and more cost effective. In the field of hydrodynamic lubrication, the flow of fluid through machine elements such as bearings, gearboxes and hydraulic systems may be governed by the Reynolds equation. The Reynolds type equations are often used in analysing the influence of surface roughness on the hydrodynamic performance of different machine elements when a lubricant is flowing through it.

The two surfaces through which a lubricant flows, may have any of the following characteristics:

(a) both surfaces are smooth and moving,

(b) both surfaces are smooth and stationary,

(c) both surfaces are rough and moving,

(d) both surfaces are rough and stationary,

(e) one surface is rough and stationary while the other is smooth and moving,

(f) one surface is rough and moving while the other is smooth and moving,

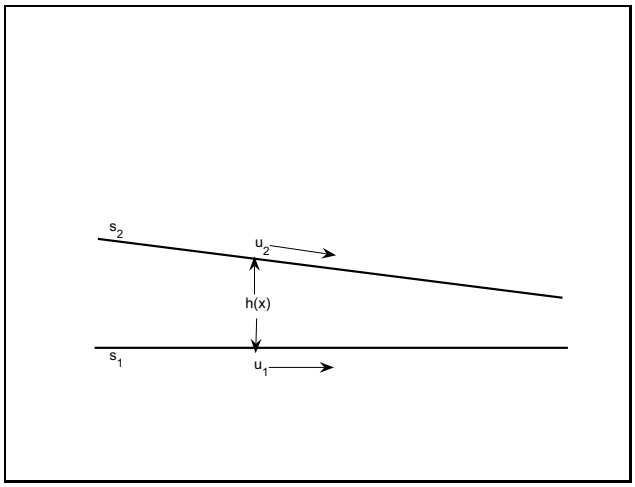

Figure 1.1: Bearing with two smooth surfaces s_1 and s_2.

(g) one surface is rough and stationary while the other is rough and moving,

(h) one surface is smooth and moving while the other is smooth and stationary, etc.

In this Licentiate thesis we will mainly consider the cases (c) and (e).

In Case (e), the governing Reynolds type equation will be time independent. This is due to the fact that the film thickness at any position x within the machine element remains the same at any time t. In Case (c), due to the motion of the rough surfaces, the governing Reynolds equation will be time dependent. As a result of this motion, the film thickness h will be changing rapidly with respect to position x and time t, thus giving rise to a rapidly oscillating (changing) lubricant pressure within the machine element. In both cases, due to the surface roughness, the coefficient h in the Reynolds equation will be oscillating rapidly and therefore we may consider the possibility of solving the problem by using an averaging process, and here homogenization theory is a very useful method.

1.1.1 Various forms of the Reynolds equations

Figure 1.1 represent the flow of liquid through two smooth bearing surfaces s_1 and s_2 with the governing Reynolds type equation given by

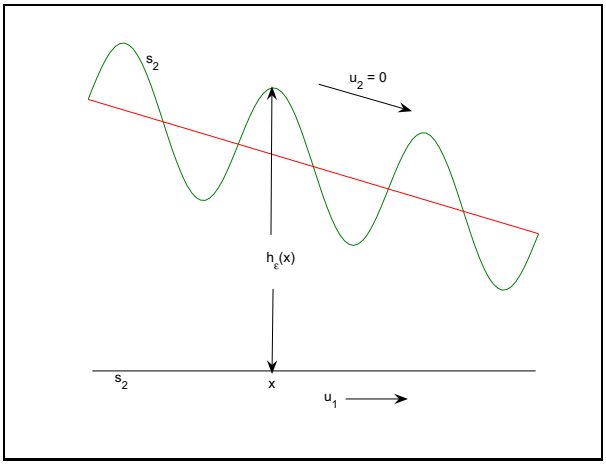

Figure 1.2: One rough stationary surface and one smooth moving surface.

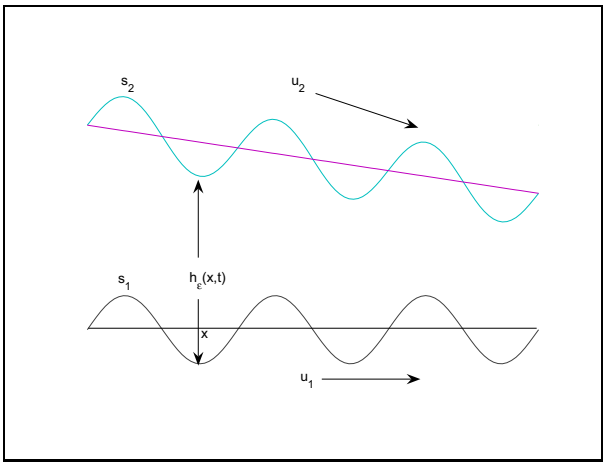

Figure 1.3: Both surfaces are rough and moving.

$$\nabla \cdot \left[\frac{\rho(p(x))h^3(x))}{12\eta} \nabla p(x) \right] = \frac{u_1 + u_2}{2} \frac{\partial}{\partial x_1} \left[\rho(p(x))h(x) \right], \qquad (1.1)$$

where u_1 and u_2 are the velocities of s_1 and s_2, respectively, η is the viscosity of the lubricant, which is assumed to be constant, whiles ρ represents the density of the lubricant, see case (a) above. Moreover, $h(x)$ is the film thickness between the two surfaces, whiles $p(x)$ is the pressure build up between the surfaces when the lubricant flows through it. The bearing domain is denoted by Ω and the space variable $x \in \Omega \subset \mathbb{R}^2$.

In general the density ρ of a lubricant is a function of the pressure, so that with a converging film thickness, we expect the pressure to be changing. This change in pressure will cause the density of the lubricant to change. Figure 1.2 is a pictorial representation of case (e) above. Due to the periodic roughness on s_2, the film thickness will depend on the roughness wavelength ε, where ε is a positive sequence converging to zero (for example $\varepsilon = \{\frac{1}{2^n}\}$ for $n = 1, 2, \cdots$). As a result of this dependence of $h(x)$ on ε, we replace $h(x)$ in (1.1) with $h_\varepsilon(x)$ to obtain the following equation:

$$\nabla \cdot \left[\frac{\rho(p_\varepsilon(x))h_\varepsilon^3(x))}{12\eta} \nabla p_\varepsilon(x) \right] = \frac{u_1 + u_2}{2} \frac{\partial}{\partial x_1} \left[\rho(p_\varepsilon(x))h_\varepsilon(x) \right], \qquad (1.2)$$

where

$$\begin{aligned} h_\varepsilon(x) &= h(x, x/\varepsilon) = h(x, y), \\ p_\varepsilon(x) &= p(x, x/\varepsilon) = p(x, y), \quad \text{for } y = x/\varepsilon. \end{aligned}$$

The variable $y = x/\varepsilon$ is called the local variable and ε obviously describes how rapid the oscillations are. We will discuss this in detail later on in this Licentiate thesis and also study what happens when $\varepsilon \to 0^+$ in a special sense.

Equation (1.2) is then the Reynolds equation, which takes into account the roughness contribution to the pressure build up in the bearing. If we assume that the rough surface is stationary, while the moving surface is smooth, then the film thickness $h_\varepsilon(x)$ at any position x within the bearing will remain the same at any time t and, hence, $h_\varepsilon(x)$ will be independent of time t. This explains why the Reynolds equation (1.2) does not involve time.

Figure 1.3 is a pictorial description of case (c) above. Here we consider the case where both surfaces are rough and moving. As a consequence of this motion, the film thickness will be changing rapidly, depending on the relative positions of the corresponding rough surfaces.

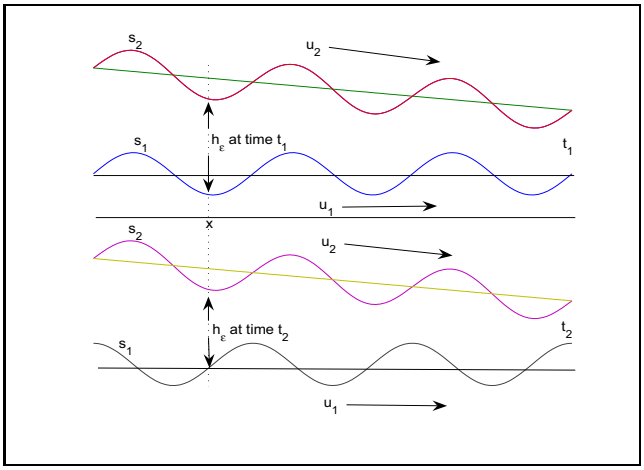

Figure 1.4: Time dependent surfaces in motion.

In Figure 1.4, we see that the film thickness h_ε at the position x is different for the two time steps t_1 and t_2. This is due to the relative positions of the corresponding rough surfaces. This shows clearly that the film thickness h_ε, which is dependent on ε, is a function of both x and t in case (c), i.e.,

$$h_\varepsilon(x,t) = h(x,t,x/\varepsilon,t/\varepsilon) = h(x,t,y,\tau),$$
$$p_\varepsilon(x,t) = p(x,t,x/\varepsilon,t/\varepsilon) = p(x,t,y,\tau),$$

where $y = x/\varepsilon$ and $\tau = t/\varepsilon$. The Reynolds equation describing such a time dependent situation is given by

$$\frac{\partial}{\partial t}\left[\rho\left(p_\varepsilon(x,t)\right) h_\varepsilon(x,t)\right] = \nabla\cdot\left[\frac{\rho\left(p_\varepsilon(x,t)\right) h_\varepsilon^3(x,t)}{12\eta}\nabla p_\varepsilon(x,t)\right] - \left(\frac{u_1+u_2}{2}\right)\frac{\partial}{\partial x_1}\left[\rho\left(p_\varepsilon(x,t)\right) h_\varepsilon(x,t)\right]. \tag{1.3}$$

In both the time independent and time dependent cases described above, we can deduce that the pressure varies rapidly due to the rapidly changing nature of the film thickness. As the roughness wavelength ε tends to zero, we expect to have a rapidly oscillating pressure. This means that we will need such a fine mesh that it is impossible to solve it directly with any numerical method. This suggests some type of averaging. One rigorous way to do this is to use the general theory of homogenization, which we

will describe, develop and use in later chapters. This theory facilitates the analysis of partial differential equations with rapidly oscillating coefficients, see e.g. Jikov et al. [21]. A more engineering oriented introduction can also be found in Persson et al. [27]. Homogenization has recently been applied to different problems connected to lubrication, see e.g. [4], [5], [7], [9], [10], [11], [13], [14], [15], [16], [19], [20], [22], [23], [25] and [28] with much success. The main aim of this Licentiate thesis is to further develop and complement these results.

The Reynolds equation can be described as being compressible or incompressible depending on the definition of $\rho\left(p_\varepsilon(x)\right)$.

If the lubricant is assumed to be incompressible, i.e. $\rho(p)$ is constant, then the equations (1.2) and (1.3) are reduced to

$$\nabla \cdot \left[h_\varepsilon^3(x)\nabla p_\varepsilon(x)\right] = \Lambda \frac{\partial h_\varepsilon(x)}{\partial x_1}, \tag{1.4}$$

$$\Gamma \frac{\partial h_\varepsilon(x,t)}{\partial t} = \nabla \cdot \left[h_\varepsilon^3(x,t)\nabla p_\varepsilon(x,t)\right] - \Lambda \frac{\partial h_\varepsilon(x,t)}{\partial x_1}, \tag{1.5}$$

where $\Gamma = 12\eta$, $\Lambda = 6\eta v$ and $v = u_1 + u_2$.

We note that the compressible equations (1.2) and (1.3) are non-linear. This means that in general it is much more difficult to analyze the compressible case. However, there is a relationship between the pressure and the density which will transform (1.2) and (1.3) respectively, into the linear forms below

$$\nabla \cdot \left(h_\varepsilon^3(x)\nabla w_\varepsilon(x)\right) = \lambda \frac{\partial}{\partial x_1}\left(w_\varepsilon(x)h_\varepsilon(x)\right), \tag{1.6}$$

$$\gamma \frac{\partial}{\partial t}\left(w_\varepsilon(x,t)h_\varepsilon(x,t)\right) = \nabla \cdot \left(h_\varepsilon^3(x,t)\nabla w_\varepsilon(x,t)\right) - \lambda \frac{\partial}{\partial x_1}\left(w_\varepsilon(x,t)h_\varepsilon(x,t)\right), \tag{1.7}$$

where $\lambda = 6\eta v\beta^{-1}$, $\gamma = 12\eta\beta^{-1}$.

These linear forms of the compressible Reynolds equations are obtained under the assumption that the dependence of density on pressure obeys the relationship

$$\rho(p_\varepsilon(x)) = \rho_a e^{(p_\varepsilon(x)-p_a)/\beta}, \tag{1.8}$$

where ρ_a is the fluid's density at the atmospheric pressure p_a and β is the bulk modulus of the fluid, which is assumed to be a positive constant. This assumption is valid for reasonably low pressures.

1.1.2 Derivation of the linear forms (1.6) and (1.7)

To further facilitate the transformation of (1.2) and (1.3) to the linear forms, we define a dimensionless density function $w_\varepsilon(x)$ as

$$w_\varepsilon(x) = \rho(p_\varepsilon(x))/\rho_a. \tag{1.9}$$

Substituting (1.8) into (1.9), we get that

$$w_\varepsilon(x) = e^{(p_\varepsilon(x)-p_a)/\beta}.$$

Hence we have that

$$\begin{aligned}\nabla w_\varepsilon(x) &= e^{(p_\varepsilon(x)-p_a)/\beta}\frac{1}{\beta}\nabla p_\varepsilon(x)\\ &= \frac{1}{\beta\rho_a}\underbrace{\rho_a e^{(p_\varepsilon(x)-p_a)/\beta}}_{\rho(p_\varepsilon(x))}\nabla p_\varepsilon(x)\\ &= \beta^{-1}\rho_a^{-1}\rho(p_\varepsilon(x))\nabla p_\varepsilon(x).\end{aligned}$$

This implies that

$$\rho_a\beta\nabla w_\varepsilon(x) = \rho(p_\varepsilon(x))\nabla p_\varepsilon(x). \tag{1.10}$$

From (1.9) we see that

$$\rho(p_\varepsilon(x)) = \rho_a w_\varepsilon(x). \tag{1.11}$$

By substituting (1.10) and (1.11) into (1.2) we obtain that

$$\nabla\cdot\left(h_\varepsilon^3(x)\nabla w_\varepsilon(x)\right) = \lambda\frac{\partial}{\partial x_1}\left(w_\varepsilon h_\varepsilon\right) \quad \text{on } \Omega,$$

where $\lambda = 6\eta v\beta^{-1}$, and (1.6) is derived.

Making similar substitutions of (1.11) and (1.10) into (1.3), we obtain the linear equation

$$\gamma\frac{\partial}{\partial t}\left(w_\varepsilon(x,t)h_\varepsilon(x,t)\right) = \nabla\cdot\left(h_\varepsilon^3(x,t)\nabla w_\varepsilon(x,t)\right) - \lambda\frac{\partial}{\partial x_1}\left(w_\varepsilon(x,t)h_\varepsilon(x,t)\right),$$

where $\gamma = 12\eta\beta^{-1}$, $\lambda = 6\eta v\beta^{-1}$ and also (1.7) is derived.

1.1.3 Outline of the homogenization procedure

Homogenization is a branch within mathematics that involves the study of PDE's with rapidly oscillating coefficients.

In deriving the homogenized Reynolds equation, we will model the lubricant film thickness in such a way that one part will describe the shape/geometry of the bearing, while the other part describes the surface roughness. The homogenized Reynolds equation describes the limiting results when the wavelength of the modelled surface roughness tends to zero (i.e. $\varepsilon \to 0^+$ in the modelling described above).

A first step to introduce and understand the homogenization of the equations (1.4) and (1.6)) is to assume multiple scale expansions of the solutions in the following forms:

$$p_\varepsilon(x) = p_0(x, \frac{x}{\varepsilon}) + \varepsilon p_1(x, \frac{x}{\varepsilon}) + \varepsilon^2 p_2(x, \frac{x}{\varepsilon}) + ...$$

and

$$w_\varepsilon(x) = w_0(x, \frac{x}{\varepsilon}) + \varepsilon w_1(x, \frac{x}{\varepsilon}) + \varepsilon^2 w_2(x, \frac{x}{\varepsilon}) + ...$$

where the functions $p_i(x, y)$ and $w_i(x, y)$, ($y = x/\varepsilon$; and $i = 0, 1, 2, ...$) are periodic in y for every $x \in \Omega$. This means that y is a "local" variable, describing the behaviour of the solution on the unit cell scale. The "global" behaviour of the solution is expressed through the variable x. The Y-periodicity means that the function is periodic in each coordinate with a period equal to the corresponding side length of Y. In this way we arrive at an equation, which yields the approximation p_0 of p_ε and w_0 of w_ε. This (more engineering oriented) approach is described in detail in chapter 2.

Chapter 2

Multiple scale expansion for Reynolds equation (stationary case)

In this chapter we will present the details concerning the multiple scale method (described in subsection 1.1.3) for deriving approximative solutions of the time independent equations (1.4) and (1.6). In each case we end up with concrete homogenization procedures, which can also be directly used by non experts in the area.

2.1 The stationary compressible (constant bulk modulus) case

The time independent compressible Reynolds equation given by (1.6), i.e.

$$\nabla \cdot \left(h_\varepsilon^3(x)\nabla w_\varepsilon(x)\right) = \lambda \frac{\partial}{\partial x_1}\left(w_\varepsilon(x)h_\varepsilon(x)\right) \quad \text{on } \Omega, \tag{2.1}$$

is used to describe the flow of thin films of fluid between two surfaces in relative motion. In this chapter we will use the method of multiple scale expansion to derive a "homogenized equation" for (2.1), which is a good approximation of (2.1) and which can be solved by using standard numerical methods. We will assume that only the stationary surface is rough.

To express the film thickness we introduce the following auxiliary function

$$h(x, y) = h_0(x) + h_1(y),$$

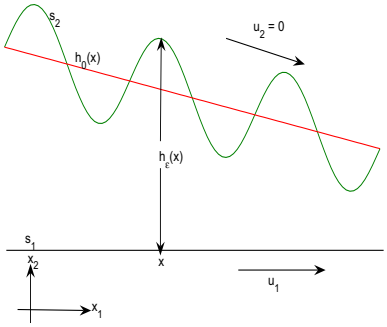

Figure 2.1: Bearing geometry and surface roughness.

where h_1 is assumed to be periodic. Without loss of generality it can also be assumed that for h_1 the cell of periodicity is $Y = (0,1) \times (0,1)$, i.e. the unit cube in $\mathbb{R}^2$. By using the auxiliary function h we can model the film thickness h_ε by

$$h_\varepsilon(x) = h(x, x/\varepsilon), \quad \varepsilon > 0.$$

This means that h_0 describes the global film thickness, the periodic function h_1, represent the roughness contribution of the surface and that ε is a parameter which describes the roughness wavelength. Further, since the coefficients $h_\varepsilon(x)$ of (2.1) are periodic functions of x/ε, it makes sense to expect that the solution is also a periodic function of its argument x/ε. Thus it is reasonable to assume a multiple scale expansion of the solution $w_\varepsilon(x)$ in the form

$$w_\varepsilon(x) = w_0(x, x/\varepsilon) + \varepsilon w_1(x, x/\varepsilon) + \varepsilon^2 w_2(x, x/\varepsilon) + ... \tag{2.2}$$

where $w_i = w_i(x, y), i = 0, 1, ...$ If $y_j = \frac{x_j}{\varepsilon}$, then applying the chain rule on the smooth function

$$\psi_\varepsilon(x) = \psi(x, x/\varepsilon),$$

the partial derivatives with respect to x_j becomes:

$$\frac{\partial \psi_\varepsilon}{\partial x_j}(x) = \left(\frac{\partial \psi}{\partial x_j} + \varepsilon^{-1} \frac{\partial \psi}{\partial y_j} \right)(x, \frac{x}{\varepsilon}), \qquad j = 1, 2. \tag{2.3}$$

Writing (2.3) in gradient form we have that

$$\nabla_x \psi_\varepsilon = \nabla_x \psi + \varepsilon^{-1} \nabla_y \psi. \tag{2.4}$$

Substituting (2.2) – (2.4) into (2.1) we obtain that

$$\begin{aligned} &\left(\nabla_x + \varepsilon^{-1}\nabla_y\right) \cdot \left[h^3 \left(\nabla_x + \varepsilon^{-1}\nabla_y\right) w_0 + \varepsilon w_1 + \varepsilon^2 w_2 + ...\right] \\ &= \lambda \left(\frac{\partial}{\partial x_1} + \varepsilon^{-1}\frac{\partial}{\partial y_1}\right)\left(hw_0 + \varepsilon h w_1 + \varepsilon^2 h w_2 + ...\right). \end{aligned} \tag{2.5}$$

To make the simplification more clear, we introduce the following notations:

$$\begin{aligned} A_0 &= \nabla_y \cdot \left(h^3 \nabla_y\right), \\ A_1 &= \nabla_y \cdot \left(h^3 \nabla_x\right) + \nabla_x \cdot \left(h^3 \nabla_y\right), \\ A_2 &= \nabla_x \cdot \left(h^3 \nabla_x\right). \end{aligned}$$

Using these notations in (2.5) we obtain that

$$\begin{aligned} &\left(\varepsilon^{-2}A_0 + \varepsilon^{-1}A_1 + A_2\right)\left(w_0 + \varepsilon w_1 + \varepsilon^2 w_2 + ...\right) \\ &= +\varepsilon^{-1}\lambda \frac{\partial}{\partial y_1}(hw_0) + \lambda\left(\frac{\partial}{\partial x_1}(hw_0) + \frac{\partial}{\partial y_1}(hw_1)\right) \\ &+ \varepsilon\lambda\left(\frac{\partial}{\partial y_1}(hw_2) + \frac{\partial}{\partial x_1}(hw_1)\right) + \varepsilon^2\lambda\frac{\partial}{\partial x_1}(hw_2) + ... \end{aligned}$$

Equating the three lowest powers of ε, we obtain the following system of equations:

$$A_0 w_0 = 0, \tag{2.6}$$

$$A_1 w_0 + A_0 w_1 = \lambda \frac{\partial}{\partial y_1}(hw_0), \tag{2.7}$$

$$A_0 w_2 + A_1 w_1 + A_2 w_0 = \lambda\left(\frac{\partial}{\partial x_1}(hw_0) + \frac{\partial}{\partial y_1}(hw_1)\right). \tag{2.8}$$

In order to solve (2.6)- (2.8), we need the following Lemma:

Lemma 2.1. *Consider the boundary value problem*

$$A_0 \Phi = F \text{ in the unit cell } Y, \tag{2.9}$$

where $F \in L^2(Y)$ and $\Phi(y)$ is Y-periodic. Then the following holds true:

(i) There exists a weak Y- periodic solution Φ of (2.9) if and only if $\frac{1}{|Y|}\int_Y F dy = 0$.

(ii) If there exists a weak Y- periodic solution of (2.9), then it is unique up to a constant, that is, if we find one solution $\Phi_0(y)$, every solution is of the form $\Phi(y) = \Phi_0(y) + c$, where c is a constant.

Proof. See [27, p. 39]. □

The operator A_0 involves only derivatives with respect to y so x is just a parameter in the solution of (2.6). One solution of (2.6) is $w_0(x,y) \equiv 0$. By Lemma 2.1, the general solution is $w_0(x,y) \equiv$ constant with respect to y, that is

$$w_0(x,y) = w_0(x). \tag{2.10}$$

In the sequel below we let

$$w_0 = w_0(x);\ w_i = w_i(x,y) \text{ for } i = 1 \text{ and } 2.$$

From (2.7) it follows that

$$A_0 w_1 = \lambda \frac{\partial}{\partial y_1}(h w_0) - A_1 w_0, \quad \text{i.e.,}$$
$$\nabla_y \cdot (h^3 \nabla_y w_1) = \lambda \frac{\partial}{\partial y_1}(h w_0) - \nabla_x \cdot \left(h^3 \nabla_y w_0\right) - \nabla_y \cdot \left(h^3 \nabla_x w_0\right).$$

According to (2.10), w_0 is a function of only x and, hence, $\nabla_y w_0$ is equal to zero. Thus we have that

$$\nabla_y \cdot \left(h^3 \nabla_y w_1\right) = \lambda \frac{\partial}{\partial y_1}(h w_0) - \nabla_y \cdot \left(h^3 \nabla_x w_0\right). \tag{2.11}$$

Since the right hand side of (2.11) consists of three (by superposition) terms, we expect that $w_1(x,y)$ should be a linear function of three terms. Hence, we let

$$w_1(x,y) = \frac{\partial w_0}{\partial x_1} v_1(x,y) + \frac{\partial w_0}{\partial x_2} v_2(x,y) + w_0 v_3(x,y). \tag{2.12}$$

In the sequel we let $v_i = v_i(x,y)$ for $i = 1, 2$ and 3. Substituting (2.12) into (2.11) we get that

$$\nabla_y \cdot \left(h^3 \nabla_y \left(\frac{\partial w_0}{\partial x_1} v_1 + \frac{\partial w_0}{\partial x_2} v_2 + w_0 v_3 \right) \right) = \lambda \frac{\partial}{\partial y_1}(h w_0) - \nabla_y \cdot \left(h^3 \nabla_x w_0\right). \tag{2.13}$$

But

$$\nabla_y \cdot \left(h^3 \nabla_x w_0\right) = \nabla_y \cdot \left(h^3 \frac{\partial w_0}{\partial x_1} e_1 + h^3 \frac{\partial w_0}{\partial x_2} e_2 \right), \tag{2.14}$$

where $\{e_1, e_2\}$ is the canonical basis in $\mathbb{R}^2$ and, hence, we can write (2.13) as

$$\nabla_y \cdot \left[h^3 \nabla_y \left(\frac{\partial w_0}{\partial x_1} v_1 + \frac{\partial w_0}{\partial x_2} v_2 + w_0 v_3 \right) \right]$$

$$= \lambda \frac{\partial}{\partial y_1}(hw_0) - \nabla_y \cdot \left(h^3 \frac{\partial w_0}{\partial x_1} e_1 + h^3 \frac{\partial w_0}{\partial x_2} e_2 \right).$$

Comparing the corresponding terms we obtain the following three local (cell) problems

$$\begin{cases} \nabla_y \cdot \left(h^3 \nabla_y v_3 \right) = \lambda \frac{\partial}{\partial y_1}(h), \\ \nabla_y \cdot \left(h^3 \nabla_y v_1 \right) = -\nabla_y \cdot \left(h^3 e_1 \right), \\ \nabla_y \cdot \left(h^3 \nabla_y v_2 \right) = -\nabla_y \cdot \left(h^3 e_2 \right). \end{cases} \tag{2.15}$$

Moreover, according to (2.8), we find that

$$A_0 w_2 + A_1 w_1 + A_2 w_0 = \lambda \frac{\partial}{\partial x_1}(hw_0) + \lambda \frac{\partial}{\partial y_1}(hw_1).$$

Averaging over the period Y we have that

$$\int_Y \left(A_0 w_2 + A_1 w_1 + A_2 w_0 - \lambda \frac{\partial}{\partial x_1}(hw_0) - \lambda \frac{\partial}{\partial y_1}(hw_1) \right) dy = 0.$$

By periodicity, $\int_Y (A_0 w_2)\, dy = 0$ and, hence, we obtain that

$$\int_Y \left(A_1 w_1 + A_2 w_0 - \lambda \frac{\partial}{\partial x_1}(hw_0) - \lambda \frac{\partial}{\partial y_1}(hw_1) \right) dy = 0,$$

or

$$\begin{aligned} &\int_Y \left[\nabla_x \cdot \left(h^3 \nabla_y w_1 \right) + \nabla_y \cdot \left(h^3 \nabla_x w_1 \right) + \nabla_x \cdot \left(h^3 \nabla_x w_0 \right) \right] dy \\ &= \int_Y \lambda \frac{\partial}{\partial x_1}(hw_0) + \lambda \frac{\partial}{\partial y_1}(hw_1) dy. \end{aligned}$$

But $h^3 \nabla_x w_1$ and hw_1 are periodic in Y so that $\int_Y \nabla_y \cdot \left(h^3 \nabla_x w_1 \right) dy = 0$, and $\int_Y \frac{\partial}{\partial y_1}(hw_1) dy = 0$. Therefore, by Lemma 2.1 the last equation reduces to

$$\begin{aligned} &\int_Y \left\{ \nabla_x \cdot \left[h^3 \nabla_y \left(w_0 v_3 + \frac{\partial w_0}{\partial x_1} v_1 + \frac{\partial w_0}{\partial x_2} v_2 \right) \right] + \right. \\ &\left. \nabla_x \cdot \left(h^3 \nabla_x w_0 \right) - \lambda \frac{\partial}{\partial x_1}(hw_0) \right\} dy = 0. \end{aligned} \tag{2.16}$$

We note that

$$\begin{cases} \nabla_x w_0 = \frac{\partial w_0}{\partial x_1} e_1 + \frac{\partial w_0}{\partial x_2} e_2, \\ \lambda \frac{\partial}{\partial x_1}(hw_0) = \nabla_x \cdot \begin{pmatrix} \lambda h w_0 \\ 0 \end{pmatrix}. \end{cases} \tag{2.17}$$

Substituting (2.17) in (2.16) and rearranging we get that

$$\begin{aligned}
&\int_Y \nabla_x \cdot \left[h^3 \nabla_y \left(\frac{\partial w_0}{\partial x_1} v_1 + \frac{\partial w_0}{\partial x_2} v_2 \right) \right] dy \\
&+ \int_Y \nabla_x \cdot \left(h^3 \frac{\partial w_0}{\partial x_1} e_1 + h^3 \frac{\partial w_0}{\partial x_2} e_2 \right) dy \\
&= \int_Y \left(\nabla_x \cdot \begin{pmatrix} \lambda h w_0 \\ 0 \end{pmatrix} - \nabla_x \cdot \left(h^3 \nabla_y w_0 v_3 \right) \right) dy.
\end{aligned}$$

By simplifying we find that

$$\begin{aligned}
&\nabla_x \cdot \left\{ \frac{\partial w_0}{\partial x_1} \int_Y \left(h^3 e_1 + h^3 \nabla_y v_1 \right) dy \right. \\
&\left. + \frac{\partial w_0}{\partial x_2} \int_Y \left(h^3 e_2 + h^3 \nabla_y v_2 \right) dy \right\} \\
&= \nabla_x \cdot \int_Y \left[\begin{pmatrix} \lambda h w_0 \\ 0 \end{pmatrix} - \begin{pmatrix} h^3 w_0 \frac{\partial v_3}{\partial y_1} \\ h^3 w_0 \frac{\partial v_3}{\partial y_2} \end{pmatrix} \right] dy,
\end{aligned}$$

or

$$\begin{aligned}
&\nabla_x \cdot \left\{ \frac{\partial w_0}{\partial x_1} \begin{pmatrix} b_{11}(x) \\ b_{21}(x) \end{pmatrix} + \frac{\partial w_0}{\partial x_2} \begin{pmatrix} b_{12}(x) \\ b_{22}(x) \end{pmatrix} \right\} \\
&= \nabla_x \cdot w_0 \begin{pmatrix} \int_Y \lambda h - h^3 \frac{\partial v_3}{\partial y_1} dy \\ \int_Y -h^3 \frac{\partial v_3}{\partial y_2} dy \end{pmatrix},
\end{aligned}$$

or

$$\nabla_x \cdot \left\{ \begin{pmatrix} b_{11}(x) & b_{12}(x) \\ b_{21}(x) & b_{22}(x) \end{pmatrix} \begin{pmatrix} \frac{\partial w_0}{\partial x_1} \\ \frac{\partial w_0}{\partial x_2} \end{pmatrix} \right\} = \nabla_x \cdot w_0 \begin{pmatrix} c_1(x) \\ c_2(x) \end{pmatrix}.$$

We conclude that the homogenized equation for (2.1) is given by

$$\nabla_x \cdot \left[B(x) \nabla w_0 \right] = \nabla_x \cdot \left[w_0 C(x) \right], \tag{2.18}$$

where $B(x)$ is a matrix function defined by $B(x) = (b_{ij}(x))$, in terms of v_1 and v_2 by

$$\begin{aligned}
\begin{pmatrix} b_{11}(x) \\ b_{21}(x) \end{pmatrix} &= \int_Y \left(h^3 e_1 + h^3 \nabla_y v_1 \right) dy, \\
\begin{pmatrix} b_{12}(x) \\ b_{22}(x) \end{pmatrix} &= \int_Y \left(h^3 e_2 + h^3 \nabla_y v_2 \right) dy,
\end{aligned} \tag{2.19}$$

and $C(x) = (c_i(x))$ is a vector function defined in terms of v_3 by

$$\begin{pmatrix} c_1(x) \\ c_2(x) \end{pmatrix} = \begin{pmatrix} \int_Y \lambda h - h^3 \frac{\partial v_3}{\partial y_1} dy \\ \int_Y -h^3 \frac{\partial v_3}{\partial y_2} dy \end{pmatrix}. \tag{2.20}$$

Note that the equation (2.18) describes the global behaviour of the solutions of (2.1) for small values of ε. Furthermore, the second term in (2.2), i.e. $\varepsilon w_1(x, x/\varepsilon)$ given by (2.7), yields important information about the local variations of the solutions, via the cell problems in (2.15) for $v_i(x, y), i = 1, 2, 3.$, and the homogenized equation (2.18) for $w_0(x)$. We end this section by summing up our investigations so far in the form of an algorithm.

Homogenization algorithm: An approximate solution of the equation (2.1) can be obtained in the following way;

step 1: Solve the *local problem* (2.15).

step 2: Insert the solution of the local problem into (2.19) and (2.20) and compute the *homogenized coefficient* $B(x)$ and the vector function $C(x)$.

step 3: Solve *the homogenized equation* (2.18), which corresponds to the approximative solution we are looking for.

We remark that all steps in this algorithm are easy to perform and, hence, we have a concrete algorithm which is easy to use in practice to solve an initially complicated problem.

2.2 The stationary incompressible case

In this section we consider multiple scale expansion of the incompressible Reynolds equation. According to (1.4) we have that

$$\nabla \cdot \left(h_\varepsilon^3(x) \nabla p_\varepsilon(x) \right) = \Lambda \frac{\partial}{\partial x_1} \left(h_\varepsilon(x) \right), \tag{2.21}$$

where $\Lambda = 6\eta v$. The parameters in the above equation have the same meanings as described in the previous section.

To express the film thickness we introduce the following auxiliary function

$$h(x, y) = h_0(x) + h_1(y),$$

where h_1 is assumed to be periodic. Without loss of generality it can also be assumed that for h_1 the cell of periodicity is $Y = (0, 1) \times (0, 1)$, i.e. the unit cube in $\mathbb{R}^2$. By using the auxiliary function h we can model the film thickness h_ε by

$$h_\varepsilon(x) = h(x, x/\varepsilon), \quad \varepsilon > 0.$$

This means that h_0 describes the global film thickness, the periodic function h_1, represent the roughness contribution of the surface and that ε is a parameter which describes the roughness wavelength

We assume a multiple scale expansion of the solution $p_\varepsilon(x)$ in the form

$$p_\varepsilon(x) = p_0(x, x/\varepsilon) + \varepsilon p_1(x, x/\varepsilon) + \varepsilon^2 p_2(x, x/\varepsilon) + ...$$

where $p_i = p_i(x, y)$ for $y = x/\varepsilon$, and $i = 1, 2, ...$ Then the chain rule (see (2.3) and (2.4)) implies that (2.21) can be written as

$$\begin{aligned} &\left(\nabla_x + \varepsilon^{-1}\nabla_y\right) \cdot \left[h^3 \left(\nabla_x + \varepsilon^{-1}\nabla_y\right) p_0 + \varepsilon p_1 + \varepsilon^2 p_2 + ...\right] \\ &= \Lambda \left(\frac{\partial}{\partial x_1} + \varepsilon^{-1}\frac{\partial}{\partial y_1}\right) h. \end{aligned} \tag{2.22}$$

For a simplification of (2.22), we introduce the following notations:

$$\begin{aligned} A_0 &= \nabla_y \cdot \left(h^3 \nabla_y\right), \\ A_1 &= \nabla_y \cdot \left(h^3 \nabla_x\right) + \nabla_x \left(h^3 \nabla_y\right), \\ A_2 &= \nabla_x \cdot \left(h^3 \nabla_x\right). \end{aligned}$$

Substituting the above notations in (2.22) we obtain that

$$\left(A_2 + \varepsilon^{-1}A_1 + \varepsilon^{-2}A_0\right)\left(p_0 + \varepsilon^{-1}p_1 + \varepsilon^{-2}p_2\right) = \Lambda \left[\frac{\partial}{\partial x_1} + \varepsilon^{-1}\frac{\partial}{\partial y_1}\right] h.$$

Expanding we have that

$$\begin{aligned} &\varepsilon^{-2}A_0p_0 + \varepsilon^{-1}\left(A_0p_1 + A_1p_0\right) + \left(A_0p_2 + A_1p_1 + A_2p_0\right) \\ &+ \varepsilon\left(A_2p_1 + A_1p_2\right) + \varepsilon^2 A_2p_2 \\ &= \Lambda \left[\frac{\partial}{\partial x_1} + \varepsilon^{-1}\frac{\partial}{\partial y_1}\right] h. \end{aligned}$$

By equating the three lowest powers of ε we get the following systems of equations:

$$A_0p_0 = 0, \tag{2.23}$$

$$A_0p_1 + A_1p_0 = \Lambda\frac{\partial h}{\partial y_1}, \tag{2.24}$$

$$A_0p_2 + A_1p_1 + A_2p_0 = \Lambda\frac{\partial h}{\partial x_1}. \tag{2.25}$$

The operator A_0 involves only derivatives with respect to y and, thus, x is just a parameter in the solution of (2.23). One solution of (2.23) is $p_0(x,y) \equiv 0$. By Lemma 2.1 the general solution $p_0(x,y) \equiv$ constant with respect to y, that is,

$$p_0(x,y) = p_0(x), \tag{2.26}$$

where $p_0(x)$ is sufficiently differentiable. In the sequel we let

$$p_0 = p_0(x);\ p_i = p_i(x,y) \quad \text{for } i = 1 \text{ and } 2.$$

In view of (2.24) we see that

$$\begin{aligned} A_0 p_1 &= \Lambda \frac{\partial h}{\partial y_1} - A_1 p_0, \text{ i.e.,} \\ \nabla_y \cdot \left(h^3 \nabla_y\right) p_1 &= \Lambda \frac{\partial h}{\partial y_1} - \nabla_x \cdot \left(h^3 \nabla_y p_0\right) - \nabla_y \cdot \left(h^3 \nabla_x p_0\right). \end{aligned}$$

Moreover, $\nabla_y p_0$ is equal to zero since, according to (2.26), p_0 is a function of only x. Thus, we have that

$$\nabla_y \cdot \left(h^3 \nabla_y p_1\right) = \Lambda \frac{\partial h}{\partial y_1} - \nabla_y \cdot \left(h^3 \nabla_x p_0\right). \tag{2.27}$$

Since the right hand side consists of three linear terms we expect that $p_1(x,y)$ should be a linear function of three terms. By linearity we let

$$p_1(x,y) = \frac{\partial p_0}{\partial x_1} v_1(x,y) + \frac{\partial p_0}{\partial x_2} v_2(x,y) + v_3(x,y). \tag{2.28}$$

Substituting (2.28) into (2.27) we get that

$$\nabla_y \cdot \left(h^3 \nabla_y \left(\frac{\partial p_0}{\partial x_1} v_1 + \frac{\partial p_0}{\partial x_2} v_2 + v_3 \right) \right) = \Lambda \frac{\partial h}{\partial y_1} - \nabla_y \cdot \left(h^3 \nabla_x p_0\right),$$

where $v_i = v_i(x,y)$ for $i = 1, 2$ and 3. But

$$\nabla_y \cdot \left[h^3 \nabla_x p_0\right] = \nabla_y \cdot \left(h^3 \frac{\partial p_0}{\partial x_1} e_1 + h^3 \frac{\partial p_0}{\partial x_2} e_2 \right),$$

and, hence, we obtain that

$$\nabla_y \cdot \left(h^3 \nabla_y \left(\frac{\partial p_0}{\partial x_1} v_1 + \frac{\partial p_0}{\partial x_2} v_2 + v_3 \right) \right) = \Lambda \frac{\partial h}{\partial y_1} - \nabla_y \cdot \left(h^3 \frac{\partial p_0}{\partial x_1} e_1 + h^3 \frac{\partial p_0}{\partial x_2} e_2 \right).$$

Comparing the corresponding terms, we obtain the following periodic problems

$$\begin{cases} \nabla_y \cdot \left(h^3 \nabla_y v_3\right) = \Lambda \frac{\partial h}{\partial y_1}, \\ \nabla_y \cdot \left(h^3 \nabla_y v_1 \frac{\partial p_0}{\partial x_1}\right) = -\nabla_y \cdot \left(h^3 \frac{\partial p_0}{\partial x_1} e_1\right), \\ \nabla_y \cdot \left(h^3 \nabla_y v_2 \frac{\partial p_0}{\partial x_2}\right) = -\nabla_y \cdot \left(h^3 \frac{\partial p_0}{\partial x_2} e_2\right), \end{cases} \tag{2.29}$$

where $v_i = v_i(x, y)$ are their solutions.

Further, averaging over the period Y in (2.25) we obtain that

$$\int_Y \left(A_0 p_2 + A_1 p_1 + A_2 p_0 - \Lambda \frac{\partial h}{\partial x_1} \right) dy = 0.$$

By periodicity $\int_Y (A_0 p_2)\, dy = 0$, and, thus, we have that

$$\int_Y \left(A_1 p_1 + A_2 p_0 - \Lambda \frac{\partial h}{\partial x_1} \right) dy = 0,$$

or

$$\int_Y \left[\nabla_x \cdot \left(h^3 \nabla_y p_1\right) + \nabla_y \cdot \left(h^3 \nabla_x p_1\right) + \nabla_x \cdot \left(h^3 \nabla_x p_0\right) - \Lambda \frac{\partial h}{\partial x_1} \right] dy = 0.$$

Since $h^3 \nabla_x p_1$ is periodic, it follows that $\int_Y \nabla_y \cdot \left(h^3 \nabla_x p_1\right) dy = 0$. Therefore the last equation reduces to

$$\begin{aligned} &\int_Y \left\{ \nabla_x \cdot \left(h^3 \nabla_y \left(\frac{\partial p_0}{\partial x_1} v_1 + \frac{\partial p_0}{\partial x_2} v_2 + v_3 \right) \right) + \right. \\ &\left. \nabla_x \cdot \left(h^3 \nabla_x p_0\right) - \Lambda \frac{\partial h}{\partial x_1} \right\} dy = 0. \end{aligned}$$

Rearranging we get that

$$\begin{aligned} &\int_Y \nabla_x \cdot \left(h^3 \nabla_y \left(\frac{\partial p_0}{\partial x_1} v_1 + \frac{\partial p_0}{\partial x_2} v_2 \right) \right) dy + \\ &\int_Y \nabla_x \cdot \left(h^3 \frac{\partial p_0}{\partial x_1} e_1 + h^3 \frac{\partial p_0}{\partial x_2} e_2 \right) dy \\ &= \int_Y \left(\Lambda \frac{\partial h}{\partial x_1} - \nabla_x \cdot \left(h^3 \nabla_y v_3\right) \right) dy. \end{aligned}$$

Simplifying we obtain that

$$\nabla_x \cdot \left\{ \frac{\partial p_0}{\partial x_1} \int_Y \left(h^3 e_1 + h^3 \nabla_y v_1\right) dy \right.$$

$$+\frac{\partial p_0}{\partial x_2}\int_Y \left(h^3 e_2 + h^3\nabla_y v_2\right) dy\Bigg\}$$
$$= \nabla_x \cdot \int_Y \left(\begin{pmatrix} \Lambda h \\ 0 \end{pmatrix} - \begin{pmatrix} h^3\frac{\partial v_3}{\partial y_1} \\ h^3\frac{\partial v_3}{\partial y_2} \end{pmatrix}\right) dy,$$

or

$$\nabla_x \cdot \left\{\frac{\partial p_0}{\partial x_1}\begin{pmatrix} b_{11}(x) \\ b_{21}(x) \end{pmatrix} + \frac{\partial p_0}{\partial x_2}\begin{pmatrix} b_{12}(x) \\ b_{22}(x) \end{pmatrix}\right\}$$
$$= \nabla_x \cdot \begin{pmatrix} \int_Y \Lambda h - h^3\frac{\partial v_3}{\partial y_1} dy \\ \int_Y -h^3\frac{\partial v_3}{\partial y_2} dy \end{pmatrix},$$

or

$$\nabla_x \cdot \left\{\begin{pmatrix} b_{11}(x) & b_{12}(x) \\ b_{21}(x) & b_{22}(x) \end{pmatrix}\begin{pmatrix} \frac{\partial p_0}{\partial x_1} \\ \frac{\partial p_0}{\partial x_2} \end{pmatrix}\right\} = \nabla_x \cdot \begin{pmatrix} c_1(x) \\ c_2(x) \end{pmatrix}. \tag{2.30}$$

In a more compact form we can write the homogenized equation (2.30) as

$$\nabla_x \cdot [B(x)\nabla p_0] = \nabla_x \cdot [c(x)], \tag{2.31}$$

where $B(x)$ is a matrix function defined by $B(x) = b_{ij}(x)$ in terms of v_1 and v_2 as

$$\begin{pmatrix} b_{11}(x) \\ b_{21}(x) \end{pmatrix} = \int_Y \left(h^3 e_1 + h^3\nabla_y v_1\right) dy, \tag{2.32}$$
$$\begin{pmatrix} b_{12}(x) \\ b_{22}(x) \end{pmatrix} = \int_Y \left(h^3 e_2 + h^3\nabla_y v_2\right) dy,$$

and the vector function $c(x) = \begin{pmatrix} c_1(x) \\ c_2(x) \end{pmatrix}$ is defined in terms of v_3 as

$$\begin{pmatrix} c_1(x) \\ c_2(x) \end{pmatrix} = \begin{pmatrix} \int_Y \Lambda h - h^3\frac{\partial v_3}{\partial y_1} dy \\ \int_Y -h^3\frac{\partial v_3}{\partial y_2} dy \end{pmatrix}. \tag{2.33}$$

Summing up, in this section we have discussed the fact that it is possible to use the method of multiple scale expansion to derive a "homogenized equation" of (2.21), which easily can be solved numerically and which gives the approximative solution we are looking for. More exactly, we can use the following:

Homogenization algorithm: An approximate solution of the equation (2.21) can be obtained in the following way;

step 1: Solve the *local problem* (2.29).

step 2: Insert the solution of the local problem into (2.32) and (2.33) and compute the *homogenized coefficient* $B(x)$ and the vector function $C(x)$.

step 3: Solve the *homogenized equation* (2.31), which corresponds to the approximative solution we are looking for.

We remark that all steps in this algorithm are easy to perform and, hence, we have a concrete algorithm which is easy to use in practice to solve an initially complicated problem.

Remark 2.1. *Also in this case it is possible to use two-scale convergence to rigorously verify that this homogenization algorithm gives the correct approximative solution we are looking for, for details see Wall [28].*

Chapter 3

Homogenization of the unstationary incompressible Reynolds equation

3.1 Introduction

To increase the hydrodynamic performance in different machine elements during lubrication, e.g. journal bearings and thrust bearings, it is important to understand the influence of surface roughness. To consider the surface effects in the numerical analysis, a very fine mesh is needed to resolve the surface roughness, suggesting some type of averaging. A rigorous way to do this is to use the general theory of homogenization. This theory facilitates the analysis of partial differential equations with rapidly oscillating coefficients, see e.g. Jikov et al. [21]. Homogenization was recently applied to different problems connected to lubrication with much success, see e.g., [4], [7], [9], [10], [11], [13], [14], [15], [16], [19], [20], [22], [23], [25] and [28].

In general, the density of a lubricant is a function of the pressure. In this paper we will consider two special cases, where the density is assumed to be constant, i.e. an incompressible lubricant, and where the compressibility of the lubricant is modelled, assuming that the lubricant has a constant bulk modulus, see e.g. [18].

If only one of the two surfaces is rough and the rough surface is stationary, then the governing Reynolds type equation is stationary. When at least one of the moving surfaces is rough, then the governing Reynolds type equations will also involve time. Most of the previous studies on the effects of

surface roughness during lubrication are devoted to problems with no time dependency.

One technique within the homogenization theory is the formal method of multiple scale expansion, see e.g. [12] or [27]. Recently, the ideas in [7] were used to study the compressible unstationary Reynolds equation under the assumption of a constant bulk modulus. In this chapter, the method of multiple scale expansion is applied to derive a homogenization result for the incompressible unstationary Reynolds equation, see also [10]. In particular, the result shows a significant difference in the asymptotic behaviors between the incompressible case and the case with constant bulk modulus. More precisely, the homogenized equation contains a fast parameter in the incompressible case. Hence the pressure distribution oscillates rapidly in time, while it is almost smooth with respect to the space variable. This is contrary to the case of constant bulk modulus where the homogenized pressure solution does not contain any fast parameters, i.e. the pressure solution is smooth in both space and time. Moreover, it is clearly demonstrated by numerical examples that the homogenization result permits the surface effects in lubrication problems to be efficiently analyzed.

We want to point out that in the more mathematical oriented works in [10] and [13], Reynolds type equations modelling roughness on both surfaces were analyzed by using the method known as two-scale convergence. Concerning the concept of two-scale convergence, the reader is also referred to e.g. [1], [24] and [26]. However, in this work we use the more engineering oriented method of multiple scale expansions.

3.2 The governing Reynolds type equations

Let η be the viscosity of the lubricant and assume that the velocity of surface i is $V_i = (v_i, 0)$, where $i = 1, 2$ and v_i is constant. Moreover, the bearing domain is denoted by Ω, the space variable is represented by $x \in \Omega \subset \mathbb{R}^2$ and $t \in I \subset \mathbb{R}$ represents the time. To express the film thickness we introduce the following auxiliary function

$$h(x, t, y, \tau) = h_0(x, t) + h_2(y - \tau V_2) - h_1(y - \tau V_1),$$

where h_1 and h_2 are assumed to be periodic. Without loss of generality it can also be assumed that for both h_1 and h_2 the cell of periodicity is $Y = (0, 1) \times (0, 1)$, i.e. the unit cube in $\mathbb{R}^2$. By using the auxiliary function h we can model the film thickness h_ε by

$$h_\varepsilon(x, t) = h(x, t, x/\varepsilon, t/\varepsilon), \quad \varepsilon > 0. \tag{3.1}$$

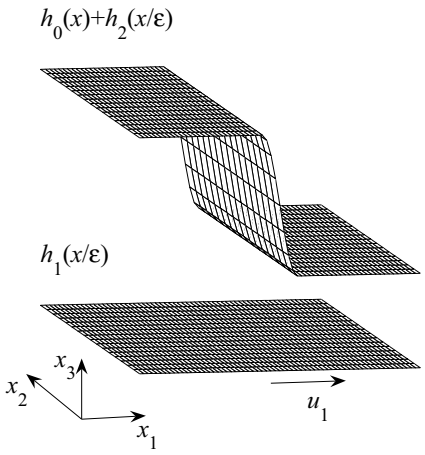

Figure 3.1: Bearing geometry and surface roughness.

This means that h_0 describes the global film thickness, the periodic functions h_i, $i = 1, 2$, represent the roughness contribution of the two surfaces and ε is a parameter that describes the roughness wavelength, see Figure 3.1.

If the lubricant is compressible, i.e. the density ρ depends on the pressure, the pressure $p(x, t)$ satisfies then the unstationary compressible Reynolds equation

$$\frac{\partial}{\partial t}\left(\rho(p_\varepsilon)h_\varepsilon\right) = \nabla \cdot \left(\frac{h_\varepsilon^3}{12\eta}\rho(p_\varepsilon)\nabla p_\varepsilon\right) - \frac{v}{2}\frac{\partial}{\partial x_1}\left(\rho(p_\varepsilon)h_\varepsilon\right), \quad \text{on } \Omega \times I, \quad (3.2)$$

where $v = v_1 + v_2$. If the lubricant is incompressible, i.e. ρ is constant, the equation (3.2) is then reduced to the unstationary incompressible Reynolds equation

$$\frac{\partial h_\varepsilon}{\partial t} = \nabla \cdot \left(\frac{h_\varepsilon^3}{12\eta}\nabla p_\varepsilon\right) - \frac{v}{2}\frac{\partial h_\varepsilon}{\partial x_1}, \quad \text{on } \Omega \times I. \quad (3.3)$$

Note that equation (3.2) is non-linear and equation (3.3) is linear. This means that in general it is much more difficult to analyze the compressible case. The situation is rather simplified if the relation between density and pressure is assumed to be of the form

$$\rho(p_\varepsilon) = \rho_a e^{(p_\varepsilon - p_a)/\beta}, \quad (3.4)$$

where the constant ρ_a is the density at the atmospheric pressure p_a and β is a positive constant (bulk modulus). This relation is equivalent to the commonly used assumption that the lubricant has a constant bulk modulus β, see e.g. [18]. Note that this assumption is valid for reasonably low pressures. Due to the special form of the relation (3.4) it is possible to transform the nonlinear equation (3.2) into a linear equation. Indeed, if the function w_ε is defined as $w_\varepsilon(x,t) = \rho(p_\varepsilon(x,t))/\rho_a$, then

$$\nabla w_\varepsilon = \beta^{-1} e^{(p_\varepsilon - p_a)/\beta} \nabla p_\varepsilon = \beta^{-1} \rho_a^{-1} \rho(p_\varepsilon) \nabla p_\varepsilon$$

and the equation (3.2) is converted into the linear equation

$$\gamma \frac{\partial}{\partial t} \left(w_\varepsilon h_\varepsilon \right) = \nabla \cdot \left(h_\varepsilon^3 \nabla w_\varepsilon \right) - \lambda \frac{\partial}{\partial x_1} \left(w_\varepsilon h_\varepsilon \right), \quad \text{on } \Omega \times I, \tag{3.5}$$

where $\gamma = 12\eta\beta^{-1}$ and $\lambda = 6\eta v \beta^{-1}$.

For small values of ε, the coefficients, including h_ε, are rapidly oscillating functions. This implies that a direct numerical analysis of the deterministic problems (3.2), (3.3) and (3.5) becomes difficult for small values of ε, because a very fine mesh is needed to resolve the surface roughness. This suggests some type of averaging. In this work, the multiple scale expansion method is used to homogenize the unstationary incompressible Reynolds equation (3.3), where h_ε is defined as in (3.1). These results will also be compared with known homogenization results for (3.5). A significant difference in the asymptotic behavior between the incompressible case and the case with constant bulk modulus will be seen.

Of note is that in the more mathematical oriented works [10] and [13] another method known as two-scale convergence was used to analyze Reynolds type equations modelling roughness on both surfaces. In particular, [13] considers air flow, where the air compressibility and slip-flow effects are considered. More precisely, the following non-linear equation is homogenized

$$a \frac{\partial}{\partial t} \left(p_\varepsilon h_\varepsilon \right) = \nabla \cdot \left(\left(h_\varepsilon^3 p_\varepsilon + b h_\varepsilon^2 \right) \nabla p_\varepsilon \right) - c \cdot \nabla \left(p_\varepsilon h_\varepsilon \right), \quad \text{on } \Omega \times I,$$

where a and b are positive constants and $c \in \mathbb{R}^2$.

3.3 Homogenization (constant bulk modulus)

The focus of this work is the homogenization of the incompressible unstationary Reynolds equation. However, the results will be compared with the

corresponding homogenization results for the unstationary equation corresponding to the constant bulk modulus case recently obtained in [7], see also [3]. Therefore, for the readers convenience, we review the main conclusions in [7].

Let χ_i, $i = 1, 2, 3$ be the solutions of the local problems

$$\nabla_y \cdot \left(h^3 \nabla_y \chi_1\right) = -\frac{\partial h^3}{\partial y_1}, \quad \text{on } Y$$

$$\nabla_y \cdot \left(h^3 \nabla_y \chi_2\right) = -\frac{\partial h^3}{\partial y_2}, \quad \text{on } Y$$

$$\nabla_y \cdot \left(h^3 \nabla_y \chi_3\right) = \gamma \frac{\partial h}{\partial \tau} + \lambda \frac{\partial h}{\partial y_1}, \quad \text{on } Y.$$

Moreover, let $\overline{h}(x,t)$, the vector function $b(x,t)$ and the matrix function $A(x,t) = (a_{ij}(x,t))$ be defined as

$$\overline{h}(x,t) = \int_T \int_Y h(x,t,y,\tau)\, dyd\tau,$$

$$b(x,t) = \int_T \int_Y \left(\lambda h e_1 - h^3 \nabla_y \chi_3\right) dyd\tau,$$

$$A(x,t) = \begin{pmatrix} \int_T \int_Y h^3 \left(1 + \dfrac{\partial \chi_1}{\partial y_1}\right) dyd\tau & \int_T \int_Y h^3 \dfrac{\partial \chi_2}{\partial y_1} dyd\tau \\ \int_T \int_Y h^3 \dfrac{\partial \chi_1}{\partial y_2} dyd\tau & \int_T \int_Y h^3 \left(1 + \dfrac{\partial \chi_2}{\partial y_2}\right) dyd\tau \end{pmatrix}.$$

The main result in [7] states that the deterministic solution w_ε of (3.5) can be approximated with high accuracy by $w_0(x,t)$, where w_0 is the solution of the homogenized (averaged) equation

$$\gamma \frac{\partial}{\partial t}\left(\overline{h} w_0\right) = -\nabla \cdot (b w_0) + \nabla \cdot (A \nabla w_0). \tag{3.6}$$

It was also clearly demonstrated that by using this homogenization result, an efficient method is obtained for analyzing the rough surface effects in problems where the lubricant has a constant bulk modulus and the governing equation is the time dependent compressible Reynolds equation (3.2).

Remark 3.1. *If h is independent of t, i.e. $h = h(x, y, \tau)$, then the homogenized equation (3.6) has the form*

$$0 = -\nabla \cdot (b w_0) + \nabla \cdot (A \nabla w_0). \tag{3.7}$$

3.4 Homogenization in the incompressible case

Consider the incompressible transient Reynolds equation

$$\Gamma \frac{\partial h_\varepsilon}{\partial t} + \Lambda \frac{\partial h_\varepsilon}{\partial x_1} - \nabla \cdot \left(h_\varepsilon^3 \nabla p_\varepsilon \right) = 0, \tag{3.8}$$

where $\Gamma = 12\eta$ and $\Lambda = 6\eta v$. Assume the following multiple scale expansion of the solution p_ε

$$p_\varepsilon = p_0 + \varepsilon p_1 + \varepsilon^2 p_2 + \cdots \tag{3.9}$$

where $p_i = p_i(x, y, t, \tau)$. The chain rule then implies that

$$\Gamma \left(\frac{\partial}{\partial t} + \frac{1}{\varepsilon} \frac{\partial}{\partial \tau} \right) h + \Lambda \left(\frac{\partial}{\partial x_1} + \frac{1}{\varepsilon} \frac{\partial}{\partial y_1} \right) h$$

$$- \left(\frac{\partial}{\partial x_i} + \frac{1}{\varepsilon} \frac{\partial}{\partial y_i} \right) \left[h^3 \left(\frac{\partial}{\partial x_i} + \frac{1}{\varepsilon} \frac{\partial}{\partial y_i} \right) (p_0 + \varepsilon p_1 + \varepsilon^2 p_2 + \cdots) \right] = 0.$$

Let $\mathcal{A}_0$, $\mathcal{A}_1$ and $\mathcal{A}_2$ be defined as

$$\mathcal{A}_0 = \frac{\partial}{\partial y_i} \left(h^3 \frac{\partial}{\partial y_i} \right) = \nabla_y \cdot \left(h^3 \nabla_y \right),$$

$$\mathcal{A}_1 = \frac{\partial}{\partial x_i} \left(h^3 \frac{\partial}{\partial y_i} \right) + \frac{\partial}{\partial y_i} \left(h^3 \frac{\partial}{\partial x_i} \right) = \nabla_x \cdot \left(h^3 \nabla_y \right) + \nabla_y \cdot \left(h^3 \nabla_x \right),$$

$$\mathcal{A}_2 = \frac{\partial}{\partial x_i} \left(h^3 \frac{\partial}{\partial x_i} \right) = \nabla_x \cdot \left(h^3 \nabla_x \right).$$

Then (3.8) may be written as

$$\Gamma \left(\frac{\partial}{\partial t} + \frac{1}{\varepsilon^1} \frac{\partial}{\partial \tau} \right) h + \Lambda \left(\frac{\partial}{\partial x_1} + \frac{1}{\varepsilon} \frac{\partial}{\partial y_1} \right) h$$

$$- \left(\varepsilon^{-2} \mathcal{A}_0 + \varepsilon^{-1} \mathcal{A}_1 + \mathcal{A}_2 \right) \left(p_0 + \varepsilon p_1 + \varepsilon^2 p_2 + \cdots \right) = 0.$$

The idea is now to collect terms of the same order of ε. For the homogenization it is sufficient to consider the orders -2, -1 and 0.

$$-\mathcal{A}_0 p_0 = 0, \tag{3.10}$$

$$\Gamma \frac{\partial h}{\partial \tau} + \Lambda \frac{\partial h}{\partial y_1} - \mathcal{A}_0 p_1 - \mathcal{A}_1 p_0 = 0, \tag{3.11}$$

$$\Gamma \frac{\partial h}{\partial t} + \Lambda \frac{\partial h}{\partial x_1} - \mathcal{A}_0 p_2 - \mathcal{A}_1 p_1 - \mathcal{A}_2 p_0 = 0. \tag{3.12}$$

It is well-known that equations of the form $\mathcal{A}_0 u = f$ has a unique solution up to an additive constant, if and only if the average over Y of the right hand side is 0, see e.g. page 93 in [2]. Hence, it is clear from (3.10) that p_0 does not depend on y, i.e. $p_0 = p_0(x,t,\tau)$. Using this fact and averaging (3.11) with respect to y gives

$$\int_Y \left(\Gamma \frac{\partial h}{\partial \tau} + \Lambda \frac{\partial h}{\partial y_1} - \nabla_y \cdot \left(h^3 \nabla_y p_1 \right) - \nabla_y \cdot \left(h^3 \nabla_x p_0 \right) \right) dy = 0.$$

By considering Y-periodicity, this is reduced to

$$\int_Y \frac{\partial h}{\partial \tau} dy = 0. \tag{3.13}$$

Hence, the assumption that p_ε may be expanded as in (3.9) requires h to satisfy (3.13). We observe that h fulfills this condition in our case. Physically this means that the surface-to-surface volume does not depend on the relative position of the surface roughness. The fact that $p_0 = p_0(x,t,\tau)$ implies that the equation (3.11) is

$$\nabla_y \cdot \left(h^3 \nabla_y p_1 \right) = \Gamma \frac{\partial h}{\partial \tau} + \Lambda \frac{\partial h}{\partial y_1} - \nabla_y \cdot \left(h^3 \nabla_x p_0 \right),$$

where x, t and τ are parameters. By linearity, p_1 is of the form

$$p_1(x,y,t,\tau) = v_1(x,y,t,\tau) + \frac{\partial p_0}{\partial x_1} v_2(x,y,t,\tau) + \frac{\partial p_0}{\partial x_2} v_3(x,y,t,\tau),$$

where v_i is the solutions of the following local problems

$$\nabla_y \cdot \left(\Lambda h e_1 - h^3 \nabla_y v_1 \right) = -\Gamma \frac{\partial h}{\partial \tau},$$

$$\nabla_y \cdot \left(h^3 (e_1 + \nabla_y v_2) \right) = 0,$$

$$\nabla_y \cdot \left(h^3 (e_2 + \nabla_y v_3) \right) = 0,$$

and $\{e_1, e_2\}$ is the canonical basis in $\mathbb{R}^2$.

Averaging the equation (3.12) with respect to y gives the equation

$$\Gamma \frac{\partial}{\partial t} \int_Y h dy + \nabla_x \cdot \int_Y \left(\Lambda h e_1 - h^3 \nabla_y v_1 \right) dy - \tag{3.14}$$

$$\nabla_x \cdot \left(\frac{\partial p_0}{\partial x_1} \int_Y h^3 \left[e_1 + \nabla_y v_2 \right] dy + \frac{\partial p_0}{\partial x_2} \int_Y h^3 \left[e_2 + \nabla_y v_3 \right] dy \right) = 0.$$

If we introduce the notation $\overline{h}(x,t,\tau) = \int_Y h dy$ and define the homogenized vector $b(x,t,\tau)$ and the homogenized matrix $A(x,t,\tau) = (a_{ij}(x,t,\tau))$ as

$$b = \int_Y \left(\Lambda h e_1 - h^3 \nabla_y v_1\right) dy,$$

$$\begin{pmatrix} a_{11} \\ a_{21} \end{pmatrix} = \int_Y h^3 (e_1 + \nabla_y v_2)\, dy \quad \text{and} \quad \begin{pmatrix} a_{12} \\ a_{22} \end{pmatrix} = \int_Y h^3 (e_2 + \nabla_y v_3)\, dy,$$

then (3.14) takes the following form:

$$\Gamma \frac{\partial \overline{h}}{\partial t}(x,t,\tau) + \nabla_x \cdot b(x,t,\tau) - \nabla_x \cdot (A(x,t,\tau)\nabla p_0) = 0. \tag{3.15}$$

Note that t and τ are just parameters. The appearance of the fast parameter τ in the homogenized equation (3.15) means that for small wavelengths the pressure will oscillate rapidly in time. This should be compared with the case of liquid flow with a constant bulk modulus, see (3.6), where the pressure is almost smooth with respect to time,. i.e. the amplitude of the oscillations in time, in the deterministic pressure solution p_ε, are very small for small wavelengths. In both cases, the pressure is almost smooth in the space variable.

It should be noted that if h is independent of t, i.e. $h = h(x,y,\tau)$, then the homogenized equation (3.15) has the form

$$\nabla_x \cdot (A(x,\tau)\nabla_x p_0(x,\tau)) = \nabla_x \cdot b(x,\tau). \tag{3.16}$$

It should also be noted that if only one of the surfaces is rough (either the moving or the stationary), i.e. h is of the form $h(x,y,t,\tau) = h_0(x,t) + h_i(y - \tau V_i)$, where $i = 1$ or $i = 2$, then $\overline{h}$, b and A are independent of τ. This means that the solution p_0 of the homogenized problem (3.15) is independent of τ and this simplifies the problem (3.15).

3.5 Numerical results

In this section we present some numerical results based on the homogenized equations obtained in the previous sections. To perform the numerical analysis, the algorithms presented in [7] and [4] are used. In all examples the solution domain Ω is a subset of $\mathbb{R}^2$ such that $0 \le x_1 \le L$ and $-L/2 \le x_2 \le L/2$. For simplicity, the global film thickness h_0 is assumed to be time independent. More precisely,

$$h_0(x) = \begin{cases} h_{\min}(1+k) & , x_1 < L/2, \\ \\ h_{\min} & , x_1 > L/2, \end{cases}$$

Parameter	Value	Unit
$h_{\min}$	$4 \cdot 10^{-6}$	m
k	$1/4$	
$c_1 = c_2$	$1/8$	
L	$1 \cdot 10^{-1}$	m
v_1	1	ms^{-1}
v_2	0	ms^{-1}
η	0.14	$Pa\ s$
β	$1 \cdot 10^{11}$	

Table 3.1: Common problem specific parameters.

and the roughness contribution is represented by

$$h_i(y - \tau v_i) = c_i h_{\min} \sin\left(2\pi\left(y - \tau v_i\right)\right).$$

This means that a step bearing with surface roughness is considered (in the numerical simulations the discontinuity has been smoothened). The specific parameters, common to all the numerical computations, may be found in Table 3.1.

3.5.1 Incompressible case

Figure 3.2 depicts the deterministic solutions p_ε of (3.8) for a fixed ε and time t. In Figure 3.3 the corresponding homogenized solution p_0 of (3.16) is plotted. It should be noted that the deterministic solution p_ε oscillates rapidly, while the homogenized solution is smooth (fixed time t and ε).

The convergence of the deterministic pressure towards the homogenized pressure p_0, as $\varepsilon \to 0$, was analyzed above by multiple scale expansions. This convergence will now be illustrated by means of numerical solutions. Indeed, Figure 3.4 represent part of the pressure distribution between the two rough surfaces along the $x_2 = 0$ line at a particular point in time for different values of ε. As seen in the figure, the pressure distribution p_ε approaches that of the homogenized pressure as ε tends to zero. Figure 3.5 represents an enlargement of a portion of Figure 3.4, showing clearly the decrease in the amplitude of the pressure distribution towards the homogenized pressure solution as the roughness wavelength ε tends to zero.

As mentioned before in the analysis by multiple scale expansions, the appearance of the fast parameter τ in the homogenized equations (3.15) and (3.16) means that for small wavelengths the pressure will oscillate rapidly in time. This fact is illustrated in Figure 3.6, which depicts the pressure

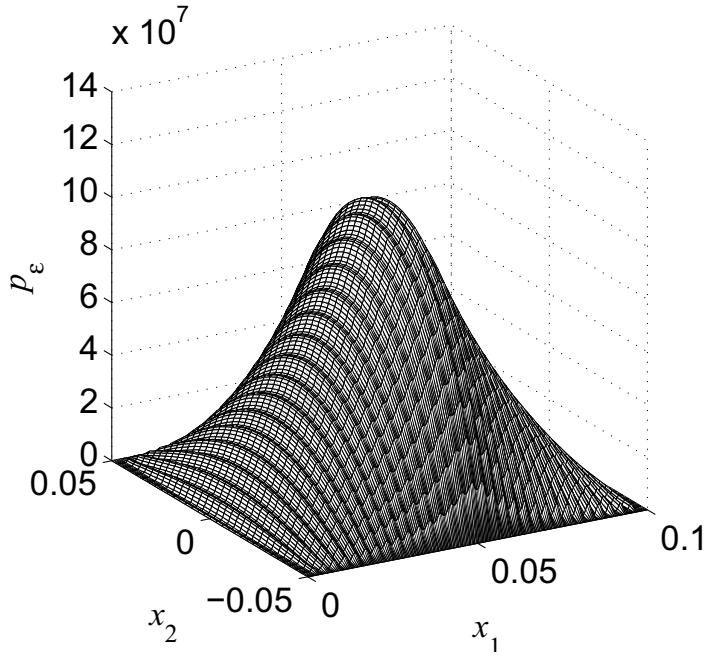

Figure 3.2: Pressure distribution in the incompressible case for a fixed ε.

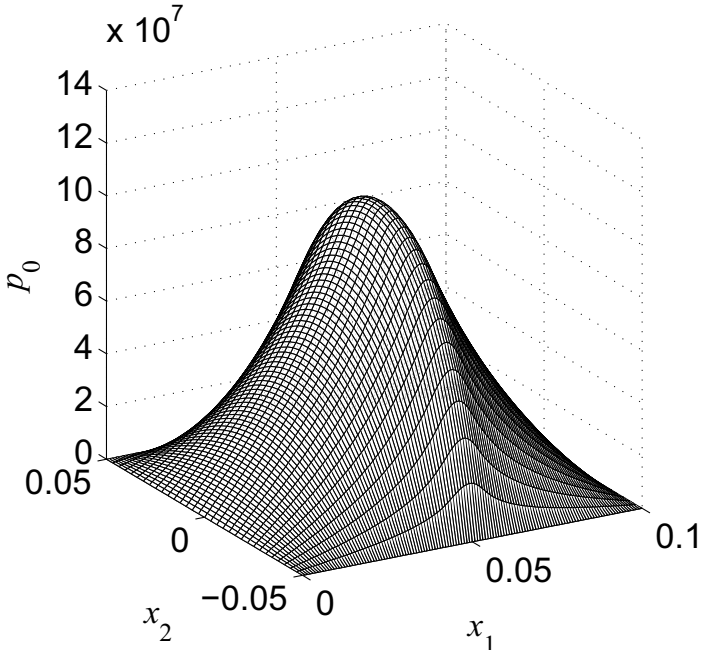

Figure 3.3: Homogenized pressure distribution for the imcompressible case.

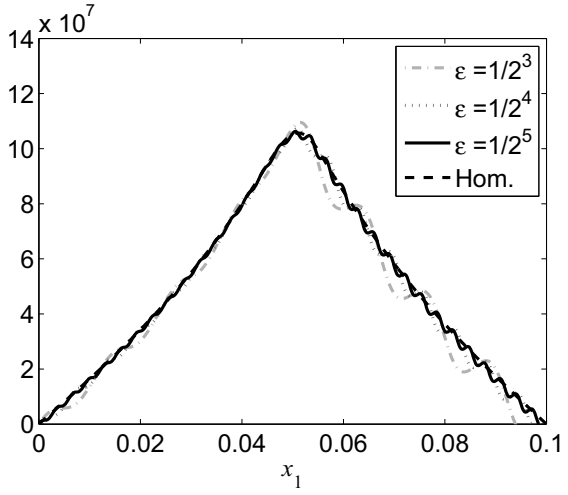

Figure 3.4: Pressure solutions at $x_2 = 0$ for various ε as well as the corresponding homogenized solution at time $t = 0$ in the incompressible case.

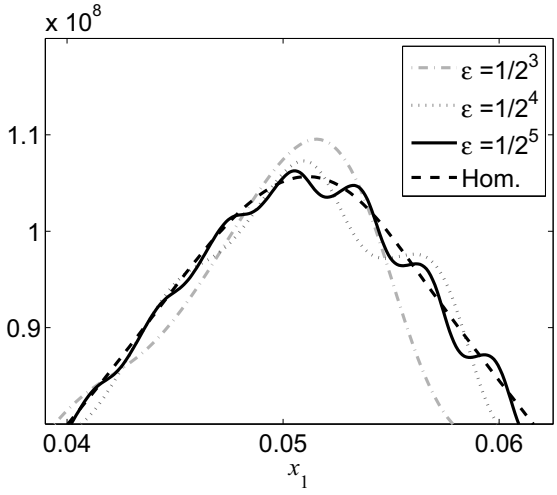

Figure 3.5: Zoomed portion of Figure 3.4.

distribution at some different times (within a period) for a fixed ε and the corresponding homogenized solutions.

In addition to the visual illustration of the convergence of p_ε to p_0, a more quantitative convergence analysis is considered here. For this purpose we consider what happens with the load carrying capacity as ε tends to 0. The load carrying capacity l_ε corresponding to p_ε and l_0 corresponding to p_0, are defined as

$$l_\varepsilon(t) = \int_\Omega p_\varepsilon(x,t)\ dx \quad \text{and} \quad l_0(\tau) = \int_\Omega p_0(x,\tau)\ dx. \tag{3.17}$$

In Figure 3.7 we see that $l_\varepsilon \to l_0$ as ε approaches zero. The difference in load carrying capacity at $t = \tau = 0$, which is the worst case scenario, is approximately 1%. It is also noted that, in the case with perfectly sinusoidal surface roughness descriptions, for a specific value of ε between 1/64 and 1/32, a seemingly small variation of the load carrying capacity in time is obtained, i.e. it is possible to optimize the surfaces to reduce vibrations.

3.5.2 Constant bulk modulus case

In the analysis by multiple scale expansions we observed a significant difference in the asymptotic behavior between the incompressible case and the case with constant bulk modulus. No fast parameter τ is found in the homogenized equation of the constant bulk modulus case. This implies that

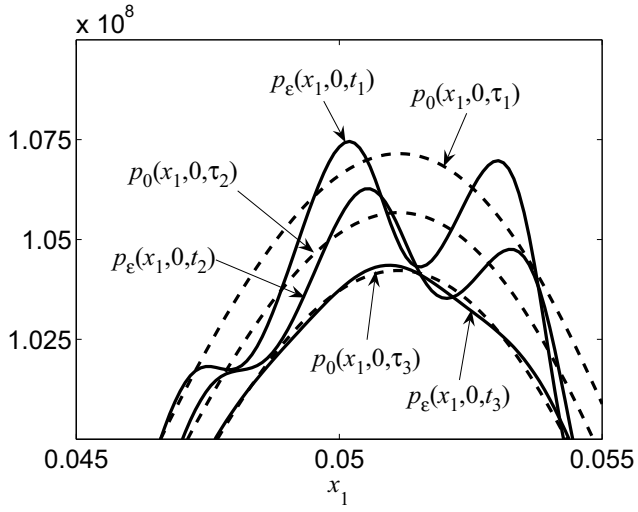

Figure 3.6: Pressure solutions at $x_2 = 0$ for three different ε as well as the corresponding homogenized solution.

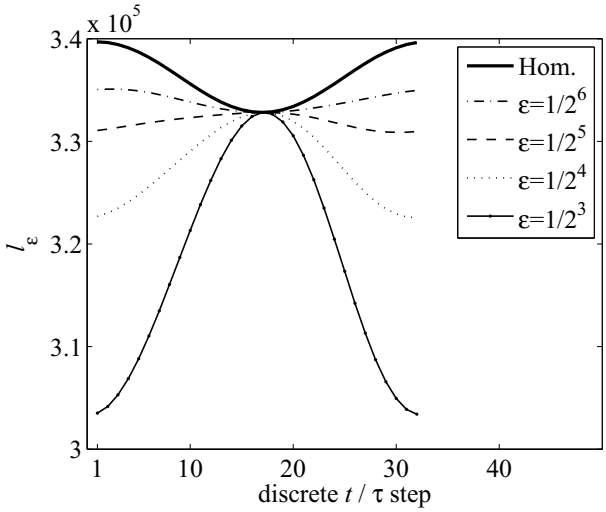

Figure 3.7: Convergence of the load carrying capacity in the incompressible case.

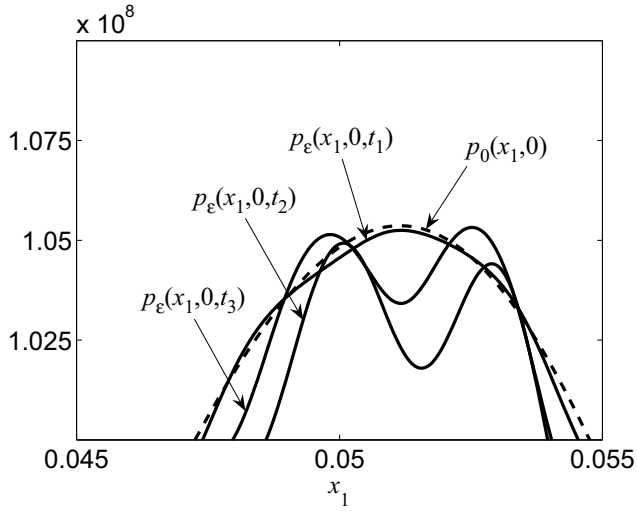

Figure 3.8: The pressure solutions for a fixed ε at three different time steps and the homogenized solution in the compressible case.

we only have one homogenized solution in our example where $h_0 = h_0(x)$ contrary to the incompressible case where we have different homogenized solutions for different times t within a period. This fact is illustrated in Figure 3.8, which corresponds to the Figure 3.6 in the incompressible situation.

In Figure 3.9 we observe that, for perfectly smooth surfaces, as β is increased, the pressure distribution in the constant bulk modulus case, approaches that in the incompressible case. However, this does not seem to be the case for rough surfaces, due to the different asymptotic behavior between the constant bulk modulus case and the incompressible case.

3.6 Concluding remarks

We have clearly demonstrated that homogenization may be used to efficiently analyze the effects of surface roughness in incompressible thin film unstationary lubrication flow. This has been done using the method of asymptotic expansions and numerical examples where we visualize the convergence and give a quantitative convergence analysis of the load capacity. One important observation is that there is a difference in the asymptotic behavior between the incompressible case and the case with constant bulk modulus. When the lubricant is assumed to be incompressible, the homogenized (averaged)

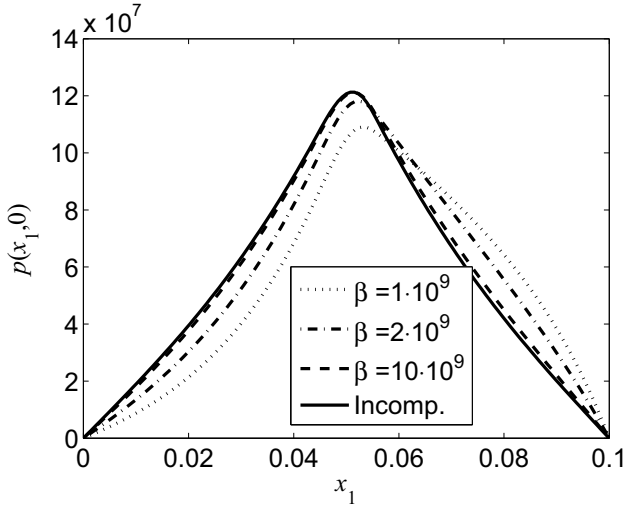

Figure 3.9: Comparison of the pressure distribution between the incompressible and compressible case when the bearing surfaces are smooth for different values of β.

equation contains a fast parameter that is connected to the time. This means that for small wavelengths the pressure distribution oscillates rapidly in time, while it is almost smooth with respect to the space variable. For liquid flow of a lubricant with a constant bulk modulus, the pressure solution of the homogenized equation does not contain any of the fast parameters. Thus, for small wavelengths the pressure is almost smooth in both the space and time variables. There are many interesting directions to deepen our study of hydrodynamic lubrication, where both surfaces are assumed to be rough. For example, to include a model that regards cavitation, another would be to consider non-Newtonian lubricants.

Chapter 4

Bounds for the unstationary Reynolds equation

The Reynolds equation describes the behavior of a thin film of lubricant separating two moving surfaces. Let $\Omega \subset \mathbb{R}^2$ be open and bounded and let $x = (x_1, x_2)$ be a cartesian coordinate system of $\mathbb{R}^2$. If the movement of the surfaces takes place in the x_1-direction only, then the pressure $p = p(x,t)$ is known to satisfy

$$\nabla \cdot \left(\frac{\rho h^3}{12\mu} \nabla p \right) = \frac{\partial}{\partial t}(\rho h) + \frac{\partial}{\partial x_1}(v \rho h) \quad \text{in } \Omega \times (0,T), \tag{4.1}$$

where ρ denotes the density of the fluid, μ the viscosity, $h = h(x,t)$ the film thickness and $v = (v_{\mathrm{U}} + v_{\mathrm{L}})/2$ the mean speed of the two surfaces, v_{U} and v_{L} denote the speeds of the upper and lower surfaces, respectively. In machine elements with rotating parts, e.g. slider bearings, polar coordinates (r, θ) may be more appropriate.

The analogue of (4.1) for polar coordinates, $p = p(r, \theta, t)$, is

$$\frac{\partial}{\partial r}\left(\frac{\rho h^3}{12\mu} r \frac{\partial p}{\partial r} \right) + \frac{\partial}{\partial \theta}\left(\frac{\rho h^3}{12\mu} \frac{1}{r} \frac{\partial p}{\partial \theta} \right) = \frac{\partial}{\partial t}(r \rho h) + \frac{\partial}{\partial \theta}(\omega r \rho h) \quad \text{in } \Omega \times (0,T), \tag{4.2}$$

where Ω is now an open bounded subset of the strip $(0, \infty) \times [0, 2\pi)$, $h = h(r, \theta, t)$ and $\omega = (\omega_{\mathrm{U}} + \omega_{\mathrm{L}})/2$ is the mean angular velocity of the surfaces.

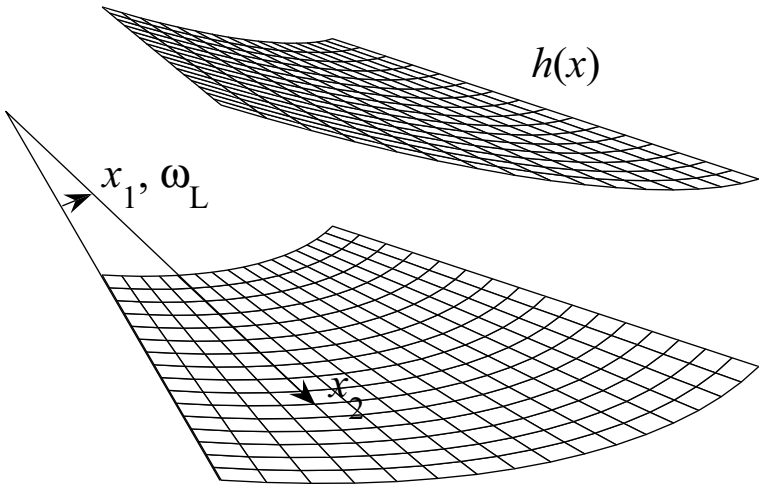

Figure 4.1: Schematics of a thrust pad bearing.

By renaming variables according to $x_1 = \theta$, $x_2 = r$ we can write (4.2) as

$$\nabla \cdot \left(\frac{\rho h^3}{12\mu} \begin{pmatrix} 1/x_2 & 0 \\ 0 & x_2 \end{pmatrix} \nabla p \right) = \frac{\partial}{\partial t}(x_2 \rho h) + \frac{\partial}{\partial x_1}(\omega x_2 \rho h) \quad \text{in } \Omega \times (0,T). \tag{4.3}$$

Figure 4.1 depicts a smooth single pad in a thrust pad bearing. The lower surface rotates with angular velocity ω_1 whiles the distance between the two surfaces is given by $h(x)$.

In this chapter an incompressible isoviscous lubricant with constant density ρ and viscosity μ is considered. This is a substantial simplification, since (4.1) and (4.3) then become linear equations.

In this work we consider (4.1) and (4.3) under the influence of periodic surface roughness. The film thickness h_ε is modelled by

$$h_\varepsilon(x,t) = h(x,t,x/\varepsilon,t/\varepsilon),$$

where $\varepsilon > 0$ is a parameter representing the roughness wavelength, while the auxiliary function $h\colon \Omega \times (0,T) \times Y \times Z \to \mathbb{R}$ is given by

$$h(x,t,y,\tau) = h_0(x,t) + h_{\mathrm{U}}(y - \tau V_{\mathrm{U}}) - h_{\mathrm{L}}(y - \tau V_{\mathrm{L}}). \tag{4.4}$$

It is assumed that $h_0\colon \Omega \times (0,T) \to \mathbb{R}$ is a contiuous function that describes the global film thickness. Moreover h_{U} and h_{L}, which represent the roughness contributions of the upper and lower surfaces, respectively, are assumed to

be periodic w.r.t. the cell Y. Without loss of generality we may assume that $Y = (0,1) \times (0,1)$. It is also assumed that v_{U} and v_{L} are such that h is periodic in τ with period Z. For simplicity it is assumed that $|Y| = |Z| = 1$, where $|\cdot|$ denotes the area or length of the corresponding periodic cell. Replacing h by h_ε in (4.1) yields

$$\nabla \cdot \left(h_\varepsilon^3 \nabla p_\varepsilon\right) = \gamma \frac{\partial h_\varepsilon}{\partial t} + \lambda \frac{\partial h_\varepsilon}{\partial x_1} \quad \text{in } \Omega \times (0,T), \tag{4.5}$$

where $\lambda = 6\mu(v_{\mathrm{U}} + v_{\mathrm{L}})$ and $\gamma = 12\mu$. By making a similar substitution in (4.3), i.e. $h_\varepsilon(x,t) = h(x,t,x/\varepsilon,t/\varepsilon)$, where h is defined as in (4.4) with $V_{\mathrm{U}} = (\omega_{\mathrm{U}}, 0)$ and $V_{\mathrm{L}} = (\omega_{\mathrm{L}}, 0)$, we obtain that

$$\nabla \cdot \left(h_\varepsilon^3 \begin{pmatrix} 1/x_2 & 0 \\ 0 & x_2 \end{pmatrix} \nabla p_\varepsilon \right) = \gamma x_2 \frac{\partial h_\varepsilon}{\partial t} + \lambda x_2 \frac{\partial h_\varepsilon}{\partial x_1} \quad \text{in } \Omega \times (0,T), \tag{4.6}$$

where $\lambda = 6\mu(\omega_{\mathrm{U}} + \omega_{\mathrm{L}})$, and $\gamma = 12\mu$.

In reality, ε is a very small number, so accurate numerical solutions of (4.5) and (4.6) may be difficult to obtain, at least at a reasonable cost, due to the rapid oscillations of h_ε, suggesting that one should study the limiting behavior of (4.5) as $\varepsilon \to 0$. Homogenization theory consists of a wide range of mathematical tools which have been devised for this purpose, see e.g. Jikov, Kozlov, Oleinik [21] or Cioranescu, Donato [17] for a survey.

Reynolds type equations have been analyzed by homogenization techniques in e.g. [6], [10], [13], [14], [15], [16],[18], and [20]. In composite engineering, it has been known for a long time that sharp bounds on the effective properties of certain composite materials exists, which can be proved by certain variational methods. In tribology, however, these techniques were only recently addressed when the stationary Reynolds equation was considered in [8] and [25]. Much work in this area still remains to be done.

The main result of this chapter is bounds for the unstationary Reynolds equations (4.5) and (4.6), thereby extending the results in [8] and [25]. Note that instead of considering (4.5) and (4.6) separately, it is more convenient to consider the following generalized form of (4.5) and (4.6)

$$\nabla \cdot (\mathbf{A}_\varepsilon \nabla p_\varepsilon) = d_\varepsilon - \nabla \cdot \mathbf{b}_\varepsilon \quad \text{in } \Omega \times (0,T), \tag{4.7}$$

where $\mathbf{A}_\varepsilon(x,t) = \mathbf{A}(x,t,x/\varepsilon,t/\varepsilon)$, $\mathbf{b}_\varepsilon(x,t) = \mathbf{b}(x,t,x/\varepsilon,t/\varepsilon)$ and $d_\varepsilon(x,t) = d(x,t,x/\varepsilon,t/\varepsilon)$. Here $\mathbf{A}$ is a diagonal matrix satisfying an ellipiticity condition, i.e. there exists $C > 0$ such that

$$\xi \cdot \mathbf{A}\xi \geq C\,|\xi|^2 \quad \forall \xi \in \mathbb{R}^2.$$

Moreover, it is a standard fact that p_ε solves (4.7) if and only if p_ε is also a solution to the variational problem

$$I_\varepsilon = \min_p \int_0^T \int_\Omega \frac{1}{2}\nabla p \cdot \mathbf{A}_\varepsilon \nabla p + \mathbf{b}_\varepsilon \cdot \nabla p + d_\varepsilon p \, dx \, dt. \tag{4.8}$$

By using the formal method of multiple scale expansions we are able to show that $I_\varepsilon \to I_0$ as $\varepsilon \to 0$, where I_0 is the minimum of some integral functional. More precisely,

$$I_0 = \min_p \int_0^T \int_\Omega \int_Z f_0(x,t,\tau,\nabla p) + d_0 p \, d\tau \, dx \, dt, \tag{4.9}$$

where

$$f_0(x,t,\tau,\xi) = \tag{4.10}$$

$$\min_w \int_Y \frac{1}{2}(\xi + \nabla w) \cdot \mathbf{A}(x,t,y,\tau)(\xi + \nabla w) + \mathbf{b}(x,t,y,\tau) \cdot (\xi + \nabla w) \, dy,$$

and $d_0(x,t,\tau) = \int_Y d(x,t,y,\tau)\, dy$.

The bounds derived in this chapter apply to the function $f_0(x,t,\tau,\cdot)$, which implies bounds on I_0. From the variational principle (4.10) an upper bound for $f_0(x,t,\tau,\cdot)$ is readily obtained. A lower bound is not so obvious, but requires a dual variational principle. The explicit results for (4.5) and (4.6) are stated at the end of this chapter.

4.1 Homogenization

By inserting the formal expression

$$p_\varepsilon(x,t) = \sum_{i=0}^{\infty} \varepsilon^i p_i(x,t,x/\varepsilon,t/\varepsilon),$$

where the functions $p_i \colon \Omega \times (0,T) \times Y \times Z \to \mathbb{R}$ are assumed to be smooth and periodic w.r.t. Y and Z, into

$$I_\varepsilon(p_\varepsilon) = \int_0^T \int_\Omega \frac{1}{2}\nabla p_\varepsilon \cdot \mathbf{A}_\varepsilon \nabla p_\varepsilon + \mathbf{b}_\varepsilon \cdot \nabla p_\varepsilon + d_\varepsilon p_\varepsilon \, dx \, dt,$$

and by applying the chain rule, one obtains the following expansion

$$I_\varepsilon(p_\varepsilon) = \varepsilon^{-2} \int_0^T \int_\Omega \frac{1}{2}\nabla_y p_0 \cdot \mathbf{A}_\varepsilon \nabla_y p_0 \, dx \; dt$$

$$
\begin{aligned}
&+\varepsilon^{-1}\int_0^T\int_\Omega \nabla_y p_0\cdot\mathbf{A}_\varepsilon(\nabla_x p_0+\nabla_y p_1)+\mathbf{b}_\varepsilon\cdot\nabla_y p_0\,dx\;dt\\
&+\int_0^T\int_\Omega \frac{1}{2}(\nabla_x p_0+\nabla_y p_1)\cdot\mathbf{A}_\varepsilon(\nabla_x p_0+\nabla_y p_1)dx\;dt\\
&+\int_0^T\int_\Omega \nabla_y p_0\cdot\mathbf{A}_\varepsilon(\nabla_x p_1+\nabla_y p_2)\\
&+\mathbf{b}_\varepsilon\cdot(\nabla_x p_0+\nabla_y p_1)+d_\varepsilon p_0\,dx\;dt+O(\varepsilon).
\end{aligned}
\tag{4.11}
$$

To proceed we need to impose some constraint on $I_\varepsilon(p_\varepsilon)$. The subsequent analysis is based on the assumption that

$$
\lim_{\varepsilon\to 0} I_\varepsilon(p_\varepsilon)<\infty. \tag{4.12}
$$

Consider the first term in the expansion (4.11), that is

$$
\varepsilon^{-2}\int_0^T\int_\Omega \frac{1}{2}\nabla_y p_0\cdot\mathbf{A}_\varepsilon\nabla_y p_0\,dx\,dt.
$$

Due to the ellipticity condition on the matrix $\mathbf{A}_\varepsilon(x,t)$, there exists a constant C such that

$$
\int_0^T\int_\Omega \frac{1}{2}\nabla_y p_0\cdot\mathbf{A}_\varepsilon\nabla_y p_0\,dx\,dt\geq C\int_0^T\int_\Omega |\nabla_y p_0|^2\,dx\,dt.
$$

By the property of the mean value, we have that

$$
\begin{aligned}
&\lim_{\varepsilon\to 0}\int_0^T\int_\Omega |\nabla_y p_0(x,t,x/\varepsilon,t/\varepsilon)|^2\,dx\,dt\\
&=\int_0^T\int_\Omega\int_Z\int_Y |\nabla_y p_0(x,t,y,\tau)|^2\,dy\,d\tau\,dx\,dt.
\end{aligned}
$$

Thus, a necessary condition for (4.12) to hold is that,

$$
\int_0^T\int_\Omega\int_Z\int_Y |\nabla_y p_0|^2\,dy\,d\tau\,dx\,dt=0.
$$

Hence $\nabla_y p_0=0$, or equivalently $p_0(x,t,y,\tau)=p_0(x,t,\tau)$. We see that (4.11) reduces to

$$
I_\varepsilon(p_\varepsilon)=\int_0^T\int_\Omega \frac{1}{2}(\nabla_x p_0+\nabla_y p_1)\cdot\mathbf{A}_\varepsilon(\nabla_x p_0+\nabla_y p_1)
$$

$$+ \mathbf{b}_\varepsilon \cdot (\nabla_x p_0 + \nabla_y p_1) + d_\varepsilon p_0 \, dx \, dt + O(\varepsilon).$$

The mean value property implies that

$$\lim_{\varepsilon \to 0} I_\varepsilon(p_\varepsilon) = \int_0^T \int_\Omega \int_Z \int_Y \frac{1}{2}(\nabla_x p_0 + \nabla_y p_1) \cdot \mathbf{A}(\nabla_x p_0 + \nabla_y p_1) + \mathbf{b} \cdot (\nabla_x p_0 + \nabla_y p_1) + d p_0 \, dy \, d\tau \, dx \, dt. \quad (4.13)$$

We remark that it is assumed that $|Y| = |Z| = 1$, but if this is not the case, then the right hand side of (4.13) must be divided by $|Y||Z|$.

The idea now is to choose p_ε so that the limit (4.13) takes the smallest possible value. Indeed, let

$$I_0 = \inf_{p_0, p_1} \int_0^T \int_\Omega \int_Z \int_Y \frac{1}{2}(\nabla_x p_0 + \nabla_y p_1) \cdot \mathbf{A}(\nabla_x p_0 + \nabla_y p_1) + \mathbf{b} \cdot (\nabla_x p_0 + \nabla_y p_1) + d p_0 \, dy \, d\tau \, dx \, dt, \quad (4.14)$$

with the infimum taken over all $p_0 \in W_0$, $p_1 \in W_{\text{per}}$, where W_0 consists of functions which are zero on the boundary and W_{per} consists of functions which are Y-periodic. We may also write

$$I_0 = \inf_p \int_0^T \int_\Omega \int_Z f_0(x, t, \tau, \nabla p) + d_0(x, t, \tau) p \, d\tau \, dx \, dt,$$

where $d_0(x, t, \tau) = \int_Y d(x, t, y, \tau) \, dy$ and $f_0 \colon \Omega \times (0, T) \times Z \times \mathbb{R}^2 \to \mathbb{R}$ is given by

$$f_0(x, t, \tau, \xi) = \inf_{w \in W_{\text{per}}} \int_Y \frac{1}{2}(\xi + \nabla w) \cdot \mathbf{A}(x, t, y, \tau)(\xi + \nabla w) + \mathbf{b}(x, t, y, \tau) \cdot (\xi + \nabla w) \, dy. \quad (4.15)$$

Thus, the multiple scale analysis suggests that

$$\min_p I_\varepsilon(p) \to \min_p \int_0^T \int_\Omega \int_Z f_0(x, t, \tau, \nabla p) + d_0(x, t, \tau) p \, d\tau \, dx \, dt \quad (4.16)$$

as $\varepsilon \to 0$. We remark that this is a result of Γ-convergence type.

4.2 Preliminaries for deriving bounds

We proceed by writing f_0 defined by (4.15) in a different form, which is suitable for obtaining bounds.

Recalling the definition of f_0

$$f_0(x,t,\tau,\xi) = \min_{w\in W_{\rm per}} \int_Y \frac{1}{2}\nabla w\cdot\mathbf{A}\nabla w + \mathbf{A}\xi\cdot\nabla w + \frac{1}{2}\xi\cdot\mathbf{A}\xi + \mathbf{b}\cdot(\xi+\nabla w)\ dy, \quad (4.17)$$

where

$$\mathbf{b} = \mathbf{b}(x,t,y,\tau) \quad \text{and} \quad \mathbf{A} = \mathbf{A}\,(x,t,y,\tau)\,.$$

We note that some of the integrals do not depend on w. Thus, if w_ξ is a minimizer of (4.17), then w_ξ is also a solution of

$$\min_{w\in W_{\rm per}} \int_Y \left(\frac{1}{2}\nabla w\cdot\mathbf{A}\nabla w + (\mathbf{A}\xi+\mathbf{b})\cdot\nabla w\right) dy. \quad (4.18)$$

This implies that the minimizer w_ξ also solves the Euler–Lagrange equation corresponding to (4.18). That is

$$\nabla_y\cdot(\mathbf{A}\nabla w_\xi + (\mathbf{A}\xi+\mathbf{b})) = 0,$$

whose weak formulation is: Find $w_\xi\in W_{\rm per}$ such that

$$\int_Y (\mathbf{A}\nabla w_\xi + (\mathbf{A}\xi+\mathbf{b}))\cdot\nabla\phi\ dy = 0 \quad \forall\phi\in W_{\rm per}.$$

By linearity it follows that w_ξ is of the form $w_\xi = v_\xi + v_0$, where v_ξ and v_0 solve the following local problems

$$\int_Y \mathbf{A}\,(\xi+\nabla v_\xi)\cdot\nabla\phi\ dy = 0, \quad (4.19)$$

$$\int_Y (\mathbf{A}\nabla v_0 + \mathbf{b})\cdot\nabla\phi\ dy = 0. \quad (4.20)$$

Hence, with $w_\xi = v_\xi + v_0$ in (4.17) we have that

$$f_0(x,t,\tau,\xi) = \int_Y \frac{1}{2}\,(\mathbf{A}\,(\xi+\nabla v_\xi))\cdot\xi + \frac{1}{2}\,(\mathbf{A}\,(\xi+\nabla v_\xi))\cdot(\nabla v_\xi+\nabla v_0) + (\mathbf{A}\nabla v_0+\mathbf{b})\cdot\xi + (\mathbf{A}\nabla v_0+\mathbf{b})\cdot(\nabla v_\xi+\nabla v_0)$$

$$-\frac{1}{2}\left(\mathbf{A}\left(\xi+\nabla v_\xi\right)\right)\cdot\nabla v_0-\frac{1}{2}\mathbf{A}\nabla v_0\cdot\nabla v_0\ dy.$$

By choosing $\phi = v_\xi$ or $\phi = v_0$ in the local problems (4.19) and (4.20) we obtain that

$$f_0(x,t,\tau,\xi)=\int_Y\frac{1}{2}\left(\mathbf{A}\left(\xi+\nabla v_\xi\right)\right)\cdot\xi+\left(\mathbf{A}\nabla v_0+\mathbf{b}\right)\cdot\xi-\frac{1}{2}\mathbf{A}\nabla v_0\cdot\nabla v_0\ dy. \tag{4.21}$$

Let the matrix function $\mathbf{A}_0(x,t,\tau)$ and vector function $\mathbf{b}_1(x,t,\tau)$ be defined via

$$\mathbf{A}_0(x,t,\tau)\xi=\int_Y\frac{1}{2}\mathbf{A}\left(\xi+\nabla v_\xi\right)dy,$$
$$\mathbf{b}_1(x,t,\tau)=\int_Y\left(\mathbf{A}\nabla v_0+\mathbf{b}\right)dy.$$

The above equations imply that

$$f_0(x,t,\tau,\xi)=\frac{1}{2}\mathbf{A}_0\xi\cdot\xi+\mathbf{b}_1\cdot\xi-\frac{1}{2}\int_Y\mathbf{A}\nabla v_0\cdot\nabla v_0\ dy.$$

From (4.20) we see that for $\phi = v_0$

$$\frac{1}{2}\int_Y\mathbf{A}\nabla v_0\cdot\nabla v_0 dy=-\frac{1}{2}\int_Y\mathbf{b}\cdot\nabla v_0 dy,$$

and, thus, we have that

$$f_0(x,t,\tau,\xi)=\frac{1}{2}\mathbf{A}_0\xi\cdot\xi+\mathbf{b}_1\cdot\xi+\frac{1}{2}\int_Y\mathbf{b}\cdot\nabla v_0 dy. \tag{4.22}$$

This gives us a formula, suitable for computation of $f_0(x,t,\tau,\xi)$.

In view of (4.16), p_0 is a solution to the minimization problem

$$\min_{p_0} I_0(p_0) =$$
$$\min_{p_0}\left\{\int_\Omega\frac{1}{2}\mathbf{A}_0\nabla p_0\cdot\nabla p_0+\mathbf{b}_1\cdot\nabla p_0+\frac{1}{2}\int_Y\mathbf{b}\cdot\nabla v_0 dy+d_0p_0\right\}dx$$

and the corresponding Euler equation

$$\nabla_x\cdot\left(\mathbf{A}_0(x,t,\tau)\nabla p_0(x,t,\tau)+\mathbf{b}_1(x,t,\tau,)\right)=d_0\ \text{ on }\Omega.$$

4.3 Bounds

In this section upper and lower bounds on a function $f\colon \mathbb{R}^2 \to \mathbb{R}$ defined by

$$f(\xi) = \min_{w \in W_{\mathrm{per}}} \int_Y \frac{1}{2}(\xi + \nabla w) \cdot \mathbf{A}(\xi + \nabla w) + \mathbf{b} \cdot (\xi + \nabla w)\, dy \tag{4.23}$$

are established, where

$$\mathbf{A}(y) = \begin{pmatrix} a_1(y) & 0 \\ 0 & a_2(y) \end{pmatrix} \quad \text{and} \quad \mathbf{b}(y) = (b_1(y), b_2(y)).$$

An estimate of the type

$$\frac{1}{2}\xi \cdot A^- \xi + b^- \cdot \xi + c^- \le f(\xi) \le \frac{1}{2}\xi \cdot A^+ \xi + b^+ \cdot \xi + c^+,$$

is proved, where $A^\pm$ is a diagonal matrix with constant coeffecients, $b^\pm$ and $c^\pm$ are constants.

4.3.1 An upper bound

Let $V = \{\phi \in W_{\mathrm{per}} : \phi(y) = \phi_1(y_1) + \phi_2(y_2)\}$. Then clearly

$$f(\xi) \le \min_{w \in V} \int_Y \frac{1}{2}(\xi + \nabla w) \cdot \mathbf{A}(\xi + \nabla w) + \mathbf{b} \cdot (\xi + \nabla w)\, dy. \tag{4.24}$$

The right hand side of (4.24) will be denoted $f^+(\xi)$ and can be calculated explicitly by solving the corresponding Euler–Lagrange equation:

$$\int_Y (\mathbf{A}(\xi + \nabla w) + \mathbf{b}) \cdot \nabla \phi \, dy = 0 \quad \forall \phi \in V. \tag{4.25}$$

Indeed, by inserting $w(y) = w_1(y_1) + w_2(y_2)$ and $\phi(y) = \phi_1(y_1) + \phi_2(y_2)$ into (4.25), we obtain that

$$\int_0^1 \left\{ \int_0^1 \big(a_1(\xi_1 + w_1') + b_1\big)\, dy_2 \right\} \phi_1'(y_1)\, dy_1 + \int_0^1 \left\{ \int_0^1 \big(a_2(\xi_2 + w_2') + b_2\big)\, dy_1 \right\} \phi_2'(y_2)\, dy_2 = 0.$$

This means that the expressions within curly brackets must be constants. Let us name these constants

$$k_1 = \int_0^1 \big(a_1(\xi_1 + w_1'(y_1)) + b_1\big)\, dy_2, \tag{4.26}$$

and

$$k_2 = \int_0^1 \big(a_2(\xi_2 + w_2'(y_2)) + b_2\big)\, dy_1. \tag{4.27}$$

But (4.26) and (4.27) imply that

$$\xi_1 + w_1' = \frac{k_1 - \int_0^1 b_1\, dy_2}{\int_0^1 a_1\, dy_2}, \tag{4.28}$$

$$\xi_2 + w_2' = \frac{k_2 - \int_0^1 b_2\, dy_1}{\int_0^1 a_2\, dy_1}. \tag{4.29}$$

In order to ease notation somewhat, let

$$A_i(y_i) = \int_0^1 a_i(y)\, dy_j \quad \text{and} \quad B_i(y_i) = \int_0^1 b_i(y)\, dy_j,$$

where i and j are complementary in $\{1, 2\}$. In this notation we have

$$k_1 = \frac{\xi_1 + \int_0^1 \frac{B_1}{A_1}\, dy_1}{\int_0^1 A_1^{-1}\, dy_1},$$

and

$$k_2 = \frac{\xi_2 + \int_0^1 \frac{B_2}{A_2}\, dy_2}{\int_0^1 A_2^{-1}\, dy_2}.$$

Now, the right hand side of (4.24) can be calculated according to

$$\begin{aligned} f^+(\xi) &= \sum_{i=1}^2 \int_0^1 \frac{A_i}{2}(\xi_i + w_i')^2 + B_i(\xi_i + w_i')\, dy_i \\ &= \sum_{i=1}^2 \int_0^1 \frac{A_i}{2}\left(\xi_i + w_i' + \frac{B_i}{A_i}\right)^2 - \frac{B_i^2}{2A_i}\, dy_i \\ &= \sum_{i=1}^2 \int_0^1 \frac{k_i^2}{2A_i} - \frac{B_i^2}{2A_i}\, dy_i \qquad \text{(by (4.28) and (4.29))} \\ &= \sum_{i=1}^2 \frac{1}{2}\frac{\left(\xi_i + \int_0^1 \frac{B_i}{A_i}\, dy_i\right)^2}{\int_0^1 A_i^{-1}\, dy_i} - \frac{1}{2}\int_0^1 \frac{B_i^2}{A_i}\, dy_i. \end{aligned} \tag{4.30}$$

Hence, if we define the matrix $\mathbf{M}$ and the vector $\mathbf{m}$ as

$$\mathbf{M}(y) = \begin{pmatrix} \int_0^1 a_1(y_1, y_2)\, dy_2 & 0 \\ 0 & \int_0^1 a_2(y_1, y_2)\, dy_1 \end{pmatrix} \text{ and } \mathbf{m} = \begin{pmatrix} \int_0^1 b_1(y_1, y_2)\, dy_2 \\ \int_0^1 b_2(y_1, y_2)\, dy_1 \end{pmatrix},$$

then we can write f^+ as

$$f^+(\xi) = \frac{1}{2}(\xi + \langle \mathbf{M}^{-1}\mathbf{m}\rangle) \cdot \langle \mathbf{M}^{-1}\rangle^{-1}(\xi + \langle \mathbf{M}^{-1}\mathbf{m}\rangle) - \frac{1}{2}\langle \mathbf{m} \cdot \mathbf{M}^{-1}\mathbf{m}\rangle,$$

where $\langle\cdot\rangle$ denotes the average with respect to Y. Or, one can write

$$f^+(\xi) = \frac{1}{2}\xi \cdot A^+\xi + b^+ \cdot \xi + c^+, \tag{4.31}$$

with

$$A^+ = \langle \mathbf{M}^{-1}\rangle^{-1}, \quad b^+ = \langle \mathbf{M}^{-1}\rangle^{-1}\langle \mathbf{M}^{-1}\mathbf{m}\rangle \quad \text{and}$$
$$c^+ = \frac{1}{2}\langle \mathbf{M}^{-1}\mathbf{m}\rangle \cdot \langle \mathbf{M}^{-1}\rangle^{-1}\langle \mathbf{M}^{-1}\mathbf{m}\rangle - \frac{1}{2}\langle \mathbf{m} \cdot \mathbf{M}^{-1}\mathbf{m}\rangle.$$

4.3.2 A dual variational principle

As a consequence of Young–Fenchel's inequality the following is true for any symmetric invertible matrix Q :

$$\frac{1}{2}u \cdot Qu + \frac{1}{2}v \cdot Q^{-1}v \geq u \cdot v \quad \forall u, v \in \mathbb{R}^2. \tag{4.32}$$

Using (4.32) pointwise with $Q = \mathbf{A}(y)$, $u = \xi + \nabla w(y)$ and $v = \sigma(y) - \mathbf{b}(y)$, where σ is any vector field on Y, we obtain that

$$f(\xi) \geq \inf_{w \in W_{\text{per}}} \int_Y \sigma \cdot (\xi + \nabla w) - \frac{1}{2}(\sigma - \mathbf{b}) \cdot \mathbf{A}^{-1}(\sigma - \mathbf{b})\, dy. \tag{4.33}$$

Let W_{sol} consist of the functions in W_{per} which have zero divergence. Then it follows from (4.33) that

$$f(\xi) \geq \sup_{\sigma \in W_{\text{sol}}} \int_Y \sigma \cdot \xi - \frac{1}{2}(\sigma - \mathbf{b}) \cdot \mathbf{A}^{-1}(\sigma - \mathbf{b})\, dy. \tag{4.34}$$

It turns out that the inequality (4.34) is actually an equality. Indeed, the solution w_ξ of the

$$\min_{w \in W_{\text{per}}} \int_Y \frac{1}{2}(\xi + \nabla w) \cdot \mathbf{A}(\xi + \nabla w) + \mathbf{b} \cdot (\xi + \nabla w)\ dy$$

is also the (unique) $w_\xi \in W_{\text{per}}$ such that

$$\int_Y (\mathbf{A}(\xi + \nabla w_\xi) + \mathbf{b}) \cdot \nabla \phi\, dy = 0 \quad \forall \phi \in W_{\text{per}}. \tag{4.35}$$

Let $\sigma^* = \mathbf{A}(\xi + \nabla w_\xi) + \mathbf{b}$. From (4.35) it is clear that σ^* belongs to W_{sol}. By choosing $\sigma = \sigma^*$ in (4.34) it is clear that we have equality in (4.34), i.e.

$$f(\xi) = \max_{\sigma \in W_{\mathrm{sol}}} \int_Y \sigma \cdot \xi - \frac{1}{2}(\sigma - \mathbf{b}) \cdot \mathbf{A}^{-1}(\sigma - \mathbf{b})\, dy.$$

From the (orthogonal) decomposition $W_{\mathrm{sol}} = \mathbb{R}^2 \oplus \mathbf{S}$, where $\mathbf{S}$ denotes the vector fields in W_{sol} with mean value zero we have that

$$\begin{aligned} f(\xi) &= \max_{\sigma \in W_{\mathrm{sol}}} \int_Y \sigma \cdot \xi - \frac{1}{2}(\sigma - \mathbf{b}) \cdot \mathbf{A}^{-1}(\sigma - \mathbf{b})\, dy \\ &= \max_{\substack{\eta \in \mathbb{R}^2 \\ \sigma \in \mathbf{S}}} \int_Y \eta \cdot \xi - \frac{1}{2}(\sigma + \eta - \mathbf{b}) \cdot \mathbf{A}^{-1}(\sigma + \eta - \mathbf{b})\, dy \\ &= \max_{\eta \in \mathbb{R}^2} \left\{ \eta \cdot \xi - \min_{\sigma \in \mathbf{S}} \int_Y \frac{1}{2}(\sigma + \eta - \mathbf{b}) \cdot \mathbf{A}^{-1}(\sigma + \eta - \mathbf{b})\, dy \right\}, \end{aligned}$$

which shows that f is the Legendre transformation (w.r.t. the variable η) of the function

$$F(\eta) = \min_{\sigma \in \mathbf{S}} \int_Y \frac{1}{2}(\sigma + \eta - \mathbf{b}) \cdot \mathbf{A}^{-1}(\sigma + \eta - \mathbf{b})\, dy.$$

In other words $f = F^*$. Since F is convex and lower semicontinuous, $(\cdot)^{**}$ acts as the identity. Thus $f^* = F^{**} = F$.

This proves the dual variational principle

$$f^*(\eta) = \min_{\sigma \in \mathbf{S}} \int_Y \frac{1}{2}(\sigma + \eta - \mathbf{b}) \cdot \mathbf{A}^{-1}(\sigma + \eta - \mathbf{b})\, dy. \tag{4.36}$$

4.3.3 A lower bound

Define the vector field space $\mathbf{S}^* \subset \mathbf{S}$ by

$$\mathbf{S}^* = \{\sigma \in \mathbf{S} : \sigma = (\sigma_1(y_2), \sigma_2(y_1))\}.$$

Obviously

$$f^*(\eta) \leq \min_{\sigma \in \mathbf{S}^*} \int_Y \frac{1}{2}(\sigma + \eta - \mathbf{b}) \cdot \mathbf{A}^{-1}(\sigma + \eta - \mathbf{b})\, dy. \tag{4.37}$$

We show that it is possible to calculate explicitly the right-hand side of (4.37) by solving the corresponding Euler–Lagrange equations: find $\sigma \in \mathbf{S}^*$ such that

$$\int_Y \begin{pmatrix} \phi_1 & 0 \\ 0 & \phi_2 \end{pmatrix} \mathbf{A}^{-1}(\sigma + \eta - \mathbf{b})\, dy = 0 \tag{4.38}$$

for all ϕ_1, ϕ_2 with mean value zero. From (4.38) we see that

$$\int_0^1 \left\{ \int_0^1 a_1^{-1}(\sigma_1(y_2) + \eta_1 - b_1)\, dy_1 \right\} \phi_1(y_2)\, dy_2 = 0.$$

By choosing $\phi_1 = \psi'$, where $\psi \in C_0^\infty(0,1)$, we can conclude that the expression between the curly brackets does not depend on y. A similar conclusion is drawn from the equation involving σ_2. Thus, we can write

$$\int_0^1 a_1^{-1}(\sigma_1 + \eta_1 - b_1)\, dy_1 = m_1, \tag{4.39}$$

$$\int_0^1 a_2^{-1}(\sigma_2 + \eta_2 - b_2)\, dy_2 = m_2, \tag{4.40}$$

where m_1 and m_2 are constants. However, (4.39) implies that

$$\begin{aligned} \sigma_1 + \eta_1 &= \left(\int_0^1 a_1^{-1}\, dy_1 \right)^{-1} \left(m_1 + \int_0^1 \frac{b_1}{a_1}\, dy_1 \right) \\ &= H_1\big(m_1 + G_1\big), \end{aligned} \tag{4.41}$$

where H_1 and G_1 (introduced to ease notation) are self-explanatory. Integration of (4.41) w.r.t. y_2 yields

$$\begin{aligned} \eta_1 &= \int_0^1 \sigma_1 + \eta_1\, dy_2 \\ &= m_1 \int_0^1 H_1\, dy_2 + \int_0^1 H_1 G_1\, dy_2, \end{aligned}$$

whence

$$m_1 = \frac{\eta_1 - \int_0^1 H_1 G_1\, dy_2}{\int_0^1 H_1\, dy_2}. \tag{4.42}$$

Similarly we can establish the relation

$$\sigma_2 + \eta_2 = H_2(m_2 + G_2), \tag{4.43}$$

where

$$m_2 = \frac{\eta_2 - \int_0^1 H_2 G_2\, dy_1}{\int_0^1 H_2\, dy_1}. \tag{4.44}$$

Note that (4.42) and(4.44) imply that

$$\int_0^1 H_i\, dy_j\, m_i^2 = \frac{\left(\eta_i - \int_0^1 H_i G_i\, dy_j\right)^2}{\int_0^1 H_i\, dy_j},$$

which will be used below.

In view of the fundamental theorem of calculus

$$\frac{(\sigma_i+\eta_i-b_i)^2}{2a_i}-\frac{b_i^2}{2a_i}=\int_0^{\sigma_i+\eta_i}\frac{(\theta-b_i)}{a_i}\,d\theta.$$

Since

$$\begin{aligned}\int_Y\int_0^{\sigma_i+\eta_i}\frac{(\theta-b_i)}{a_i}\,d\theta\,dy&=\int_0^1\int_0^{\sigma_i(y_j)+\eta_i}\int_0^1\frac{(\theta-b_i)}{a_i}\,dy_i\,d\theta\,dy_j\\&=\int_0^1\int_0^{H_i(m_i+G_i)}\frac{\theta}{H_i}-G_i\,d\theta\,dy_j\\&=\int_0^1\left[\frac{\theta^2}{2H_i}-G_i\theta\right]_0^{H_i(m_i+G_i)}dy_j\\&=\int_0^1\frac{1}{2}H_i(m_i+G_i)^2-G_iH_i(m_i+G_i)\,dy_j\\&=\frac{1}{2}\int_0^1 H_i\,dy_j\,m_i^2-\frac{1}{2}\int_0^1 H_iG_i^2\,dy_j\\&=\frac{\left(\eta_i-\int_0^1 H_iG_i\,dy_j\right)^2}{2\int_0^1 H_i\,dy_j}-\frac{1}{2}\int_0^1 H_iG_i^2\,dy_j,\end{aligned}$$

we find that

$$\begin{aligned}\int_Y\frac{(\sigma_i+\eta_i-b_i)^2}{2a_i}\,dy=&\frac{\left(\eta_i-\int_0^1 H_iG_i\,dy_j\right)^2}{2\int_0^1 H_i\,dy_j}\\&-\frac{1}{2}\int_0^1 H_iG_i^2\,dy_j+\int_Y\frac{b_i^2}{2a_i}\,dy.\end{aligned}$$

Thus, we obtain that

$$f^{*+}(\eta)=\sum_{i=1}^2\frac{\left(\eta_i-\int_0^1 H_iG_i\,dy_j\right)^2}{2\int_0^1 H_i\,dy_j}+\int_Y\frac{b_i^2}{2a_i}dy-\frac{1}{2}\int_0^1 H_iG_i^2\,dy_j.$$

Let

$$\mathbf{N}(y)=\begin{pmatrix}\int_0^1 a_1(y_1,y_2)^{-1}\,dy_1 & 0\\ 0 & \int_0^1 a_2(y_1,y_2)^{-1}\,dy_2\end{pmatrix}^{-1}=\begin{pmatrix}H_1(y_2) & 0\\ 0 & H_2(y_1)\end{pmatrix},$$

and

$$\mathbf{n}(y) = \left(\int_0^1 \tfrac{b_1}{a_1}(y_1, y_2)\, dy_1, \quad \int_0^1 \tfrac{b_2}{a_2}(y_1, y_2)\, dy_2\right) = \big(G_1(y_2), G_2(y_1)\big)\,.$$

Then

$$f^{*+}(\eta) = \frac{1}{2}(\eta - \langle \mathbf{Nn}\rangle)\cdot\langle \mathbf{N}\rangle^{-1}(\eta - \langle \mathbf{Nn}\rangle) + \frac{1}{2}\langle \mathbf{b}\cdot\mathbf{A^{-1}b}\rangle - \frac{1}{2}\langle \mathbf{n}\cdot\mathbf{Nn}\rangle.$$

The conjugate function of f^{*+} is

$$f^{*+*}(\xi) = \frac{1}{2}\xi\cdot\langle \mathbf{N}\rangle\xi + \langle \mathbf{Nn}\rangle\cdot\xi + \frac{1}{2}\langle \mathbf{n}\cdot\mathbf{Nn}\rangle - \frac{1}{2}\langle \mathbf{b}\cdot\mathbf{A^{-1}b}\rangle.$$

Hence, if $A^- = \langle \mathbf{N}\rangle$, $b^- = \langle \mathbf{Nn}\rangle$ and $c^- = \frac{1}{2}\langle \mathbf{n}\cdot\mathbf{Nn}\rangle - \frac{1}{2}\langle \mathbf{b}\cdot\mathbf{A^{-1}b}\rangle$, then f is bounded from below by the function

$$f^-(\xi) = \frac{1}{2}\xi\cdot A^-\xi + b^-\cdot\xi + c^-. \tag{4.45}$$

4.3.4 Reuss–Voigt bounds

To obtain a bound on f we choose w as a constant in the right hand side of (4.23). Indeed

$$f(\xi) \le \int_Y \frac{1}{2}\xi\cdot\mathbf{A}\xi + \mathbf{b}\cdot\xi\, dy = \frac{1}{2}\xi\cdot\langle\mathbf{A}\rangle\xi + \langle\mathbf{b}\rangle\cdot\xi.$$

Similarly, in view of the dual variational principle (4.36),

$$\begin{aligned} f^*(\eta) &\le \int_Y \frac{1}{2}(\eta - \mathbf{b})\cdot\mathbf{A}^{-1}(\eta - \mathbf{b})\, dy \\ &= \frac{1}{2}\eta\cdot\langle\mathbf{A}^{-1}\rangle\eta - \eta\cdot\langle\mathbf{A}^{-1}\mathbf{b}\rangle + \frac{1}{2}\langle\mathbf{b}\cdot\mathbf{A}^{-1}\mathbf{b}\rangle. \end{aligned}$$

We compute the Legendre transformation of

$$\begin{aligned} &\frac{1}{2}\eta\cdot\langle\mathbf{A}^{-1}\rangle\eta - \eta\cdot\langle\mathbf{A}^{-1}\mathbf{b}\rangle + \frac{1}{2}\langle\mathbf{b}\cdot\mathbf{A}^{-1}\mathbf{b}\rangle \overset{*}{\mapsto} \\ &\qquad\qquad \frac{1}{2}(\xi + \langle\mathbf{A}^{-1}\mathbf{b}\rangle)\cdot\langle\mathbf{A}^{-1}\rangle^{-1}(\xi + \langle\mathbf{A}^{-1}\mathbf{b}\rangle) - \frac{1}{2}\langle\mathbf{b}\cdot\mathbf{A}^{-1}\mathbf{b}\rangle, \end{aligned}$$

which we define as the lower Reuss–Voigt bound on f. Thus, the estimate $f^-_{\mathrm{RV}} \le f \le f^+_{\mathrm{RV}}$ holds, where

$$\begin{aligned} f^-_{\mathrm{RV}}(\xi) = &\frac{1}{2}\xi\cdot\langle\mathbf{A}^{-1}\rangle^{-1}\xi + \xi\cdot\langle\mathbf{A}^{-1}\rangle^{-1}\langle\mathbf{A}^{-1}\mathbf{b}\rangle \\ &+ \frac{1}{2}\langle\mathbf{A}^{-1}\mathbf{b}\rangle\cdot\langle\mathbf{A}^{-1}\rangle^{-1}\langle\mathbf{A}^{-1}\mathbf{b}\rangle - \frac{1}{2}\langle\mathbf{b}\cdot\mathbf{A}^{-1}\mathbf{b}\rangle, \end{aligned}$$

and

$$f^+_{\mathrm{RV}}(\xi) = \frac{1}{2}\xi\cdot\langle\mathbf{A}\rangle\xi + \langle\mathbf{b}\rangle\cdot\xi.$$

4.4 Application to a problem in hydrodynamic lubrication

In this section the Reuss–Voigt and the arithmetic-harmonic bounds are applied to a lubrication problem, i.e. the hydrodynamic lubrication of a thrust pad bearing, see Figure 4.1 for a schematic description of a single pad.

By the chain rule and (4.4), it follows that the function h_ε in (4.6) satisfies

$$\frac{\partial h_\varepsilon}{\partial t}(x,t) = \frac{\partial h_0}{\partial t}(x,t) + \omega_{\mathrm{L}} \frac{\partial}{\partial x_1} h_{\mathrm{L}}(x/\varepsilon, t/\varepsilon) - \omega_{\mathrm{U}} \frac{\partial}{\partial x_1} h_{\mathrm{U}}(x/\varepsilon, t/\varepsilon). \quad (4.46)$$

Define an auxiliary function $\widetilde{h}$ as

$$\widetilde{h}(x,t,y,\tau) = h(x,t) + \frac{\gamma}{\lambda}\left(\omega_{\mathrm{L}} h_{\mathrm{L}}(x/\varepsilon, t/\varepsilon) - \omega_{\mathrm{U}} h_{\mathrm{U}}(x/\varepsilon, t/\varepsilon)\right). \quad (4.47)$$

A physical interpretation of $\widetilde{h}$ is more apparent if it is expressed as

$$\widetilde{h}(x,t,y,\tau) = h_0(x,t) + S\frac{h_{\mathrm{L}}(x/\varepsilon, t/\varepsilon) + h_{\mathrm{U}}(x/\varepsilon, t/\varepsilon)}{2}, \quad (4.48)$$

where the slide-to-roll ratio S, defined by

$$S = 2\frac{\omega_{\mathrm{L}} - \omega_{\mathrm{U}}}{\omega_{\mathrm{L}} + \omega_{\mathrm{U}}},$$

has been introduced. The right hand side of (4.6) may be expressed in terms of $\widetilde{h}$ according to:

$$\lambda \frac{\partial h_\varepsilon}{\partial x_1} + \gamma \frac{\partial h_\varepsilon}{\partial t} =$$

$$= \lambda \frac{\partial \widetilde{h}}{\partial x_1} + \gamma \frac{\partial h_0}{\partial t} =$$

$$= \lambda \frac{\partial h_0}{\partial x_1} + \gamma \frac{\partial h_0}{\partial t} + S\frac{\partial}{\partial x_1}\left(\frac{h_{\mathrm{L}} + h_{\mathrm{U}}}{2}\right).$$

From this expression it is clear that the contribution from surface roughness to hydrodynamic pressure build-up acts through the x_1-direction. More precisely, it acts through the x_1-direction derivative of the mean value of the rough surfaces and the slide-to-roll ratio S.

Thus (4.6) may be written in the general form (4.7) by taking

$$\mathbf{A}(x,t,y,\tau) = h(x,t,y,\tau)^3 \begin{pmatrix} 1/x_2 & 0 \\ 0 & x_2 \end{pmatrix},$$

$$\mathbf{b}(x,t,y,\tau) = -\lambda x_2 \widetilde{h}(x,t,y,\tau) e_1,$$
$$d_0(x,t) = \gamma x_2 \frac{\partial h_0}{\partial t}(x,t).$$

Define

$$\begin{aligned}
A^+(x,t,\tau) &= \left\langle \mathcal{A}^+(x,t,\cdot,\tau)^{-1} \right\rangle^{-1}, \\
b^+(x,t,\tau) &= A^+(x,t,\tau) \left\langle \left(\mathcal{A}^+\right)^{-1} \beta^+(x,t,\cdot,\tau) \right\rangle, \\
c^+ &= \frac{1}{2} \langle \left(\mathcal{A}^+\right)^{-1} \beta^+(x,t,\cdot,\tau) \rangle \\
&\quad \cdot \langle \mathcal{A}^+(x,t,\cdot,\tau)^{-1} \rangle^{-1} \langle \left(\mathcal{A}^+\right)^{-1} \beta^+(x,t,\cdot,\tau) \rangle \\
&\quad - \frac{1}{2} \langle \beta^+ \cdot \left(\mathcal{A}^+\right)^{-1} \beta^+(x,t,\cdot,\tau) \rangle \\
A^-(x,t,\tau) &= \left\langle \mathcal{A}^-(x,t,\cdot,\tau) \right\rangle, \\
b^-(x,t,\tau) &= \left\langle \beta^-(x,t,\cdot,y) \right\rangle, \\
c^- &= \frac{1}{2} \langle \beta^- \cdot \mathcal{A}^- \beta^-(x,t,\cdot,\tau) \rangle - \frac{1}{2} \langle \mathbf{b} \cdot \mathbf{A^{-1}} \mathbf{b}(x,t,\cdot,\tau) \rangle
\end{aligned} \tag{4.49}$$

where

$$\mathcal{A}^+(x,t,y,\tau) = \begin{pmatrix} \int_0^1 a_1(x,t,y,\tau)\, dy_2 & 0 \\ 0 & \int_0^1 a_2(x,t,y,\tau)\, dy_1 \end{pmatrix},$$
$$\mathcal{A}^-(x,t,y,\tau) = \begin{pmatrix} \int_0^1 a_1(x,t,y,\tau)^{-1}\, dy_1 & 0 \\ 0 & \int_0^1 a_2(x,t,y,\tau)^{-1}\, dy_2 \end{pmatrix}^{-1},$$
$$\beta^+(x,t,y,\tau) = \begin{pmatrix} \int_0^1 b_1(x,t,y,\tau)\, dy_2 \\ \int_0^1 b_2(x,t,y,\tau)\, dy_1 \end{pmatrix},$$

$$\beta^-(x,t,y,\tau) = \mathcal{A}^-(x,t,y,\tau) \begin{pmatrix} \int_0^1 \frac{b_1}{a_1}(x,t,y,\tau)\, dy_1 \\ \int_0^1 \frac{b_2}{a_2}(x,t,y,\tau)\, dy_2 \end{pmatrix}.$$

The bounds (4.31) and (4.45) imply that $I_0^- \le I_0 \le I_0^+$, where

$$I_0^\pm = \min_p \int_\Omega \frac{1}{2} \nabla p \cdot A^\pm \nabla p + b^\pm \cdot \nabla p + c^\pm + d_0\ p\ dx. \tag{4.50}$$

The Euler–Lagrange equations corresponding to (4.50) are given by

$$\nabla \cdot \left(A^\pm \nabla p^\pm\right) = d_0 - \nabla \cdot b^\pm. \tag{4.51}$$

The relation

$$\frac{\partial h_\varepsilon}{\partial t}(x,t) = \frac{\partial h_0}{\partial t}(x,t) + v_{\mathrm{L}}\frac{\partial}{\partial x_1}h_{\mathrm{L}}(x/\varepsilon, t/\varepsilon) - v_{\mathrm{U}}\frac{\partial}{\partial x_1}h_{\mathrm{U}}(x/\varepsilon, t/\varepsilon)$$

is easily verified by using the chain rule.

It is observed that (4.5) is a special case of (4.7) by taking

$$\begin{aligned}
\mathbf{A}(x,t,y,\tau) &= h(x,t,y,\tau)^3 \begin{pmatrix} 1 & 0 \\ 0 & 1 \end{pmatrix}, \\
\mathbf{b}(x,t,y,\tau) &= -\lambda\widetilde{h}(x,t,y,\tau)(1,0), \\
\widetilde{h}(x,t,y,\tau) &= h_0(x,t) + \frac{v_{\mathrm{L}} - v_{\mathrm{U}}}{v_{\mathrm{L}} + v_{\mathrm{U}}}(h_{\mathrm{U}}(y,\tau) + h_{\mathrm{L}}(y,\tau)), \\
d_0(x,t) &= \gamma\frac{\partial h_0}{\partial t}(x,t).
\end{aligned}$$

If we define $A^{\pm}$ and $b^{\pm}$ as in (4.49), then we find that, results similar to (4.50) and (4.51) holds.

Note: The coefficients in the Euler–Lagrange equation corresponding to the Reuss–Voigt bounds are:

$$\begin{aligned}
A^-_{\mathrm{RV}}(x,t,\tau) &= \langle \mathbf{A}(x,t,\cdot,\tau)^{-1}\rangle^{-1}, \quad & b^-_{\mathrm{RV}}(x,t,\tau) &= A^-_{\mathrm{RV}}(x,t,\tau)\langle \mathbf{A}^{-1}\mathbf{b}(x,t,\cdot,\tau)\rangle, \\
A^+_{\mathrm{RV}}(x,t,\tau) &= \langle \mathbf{A}(x,t,\cdot,\tau)\rangle, & b^+_{\mathrm{RV}}(x,t,\tau) &= \langle \mathbf{b}(x,t,\cdot,\tau)\rangle.
\end{aligned}$$

4.4.1 Numerical results and discussion

All numerical simulations performed relies on the assumption that $h = h(x,y,\tau)$, is of the following form:

$$h(x,y,\tau) = h_0(x) + h_{\mathrm{U}}(y,\tau) - h_{\mathrm{L}}(y,\tau). \tag{4.52}$$

Further, the results are dimensionless, i.e., the following dimensionless variables are used:

$$X_2 = x_2/x_{2r}, \quad H = h/h_r, \quad P = p/p_r.$$

Since the simulations concern a thrust pad bearing, the radius of the inner pad R_1 is used as the scaling parameter (i.e. $x_{2r} = R_1$; $1 \le X_2 \le R_2/R_1$). The film thickness h_{00} at the trailing edge is also used to represent the scaling parameter h_r (i.e. $h_r = h_{00}$). If the surfaces are perfectly smooth then h_{00} represents the minimum film thickness. The dimensionless global film thickness H_0 is given by

$$H_0(X) = 1 - KX_2\frac{R_1}{R_2}\frac{\sin X_1 - \sin\theta_2}{\sin\theta_2 - \sin\theta_1},$$

where $R_1/R_2 = 3/7$, $\theta_2 = -\theta_1 = 27.5^\circ$ and $K = 1/4$. These values are used in simulating a single pad in a thrust pad bearing which is assumed to have 6 pads separated by an angle of 5° and operating at 1/4 inclination with $R_1/R_2 = 3/7$.

To make the pressure dimensionless we introduce the following scaling parameter

$$p_r = \frac{6\mu\left(\omega_{\mathrm{L}} + \omega_{\mathrm{U}}\right) R_1}{h_{00}^2}.$$

This choice together with the film thickness given by (4.52) transforms (4.6) to

$$\nabla \cdot \left(H_\varepsilon^3 \begin{pmatrix} 1/X_2 & 0 \\ 0 & X_2 \end{pmatrix} \nabla w_\varepsilon \right) = X_2 \frac{\partial \widetilde{H}_\varepsilon}{\partial X_1}, \tag{4.53}$$

where $\nabla = \left(\partial/\partial X_1, \partial/\partial X_2\right)$. This is a convenient form, since it does not contain any reference or input parameters. By solving this equation once, for a given R_1/R_2, k and for a specific surface roughness representation $\left(h_{\mathrm{U}}\left(y,\tau\right) - h_{\mathrm{L}}\left(y,\tau\right)\right)$ we have simulated a 6 pad bearing, with pads separated by an angle of 5° for any given choice of parameters μ, $\left(\omega_{\mathrm{L}} + \omega_{\mathrm{U}}\right)$, R_1 and h_{00}.

In the next section we present some illustrative cases of the simulations performed using the above equations.

4.4.2 Sinusoidal roughness

In the first problem to be considered, both the upper and lower surfaces have a one-dimensional sinusoidal roughness and the upper surface is assumed to be stationary i.e $\omega_{\mathrm{U}} = 0$. More precisely, the roughness is described by

$$\begin{aligned} H_{\mathrm{U}}\left(y_1,\tau\right) &= -\frac{c}{2}\left(\sin\left(2\pi y_1\right) - 1\right), \\ H_{\mathrm{L}}\left(y_1,\tau\right) &= \frac{c}{2}\left(\sin\left(2\pi\left(y_1 - \omega_{\mathrm{L}}\tau\right)\right) - 1\right), \end{aligned} \tag{4.54}$$

where $c = 1/8$ and $\omega_{\mathrm{L}} = 100$ RPM $= 100\pi/30$ rad/s. In Figure 4.2 the dimensionless deterministic pressure distribution corresponding to the surface roughness representation (4.54) is visualized. The bounds pressure solutions numerically coincides with each other as expected, when the roughness only depends on one of the variables. We now introduce a measure of the difference between the upper/lower bound and the homogenized solution which may be used to quantify the accurracy. We remark that the solution(s) are periodic in τ.

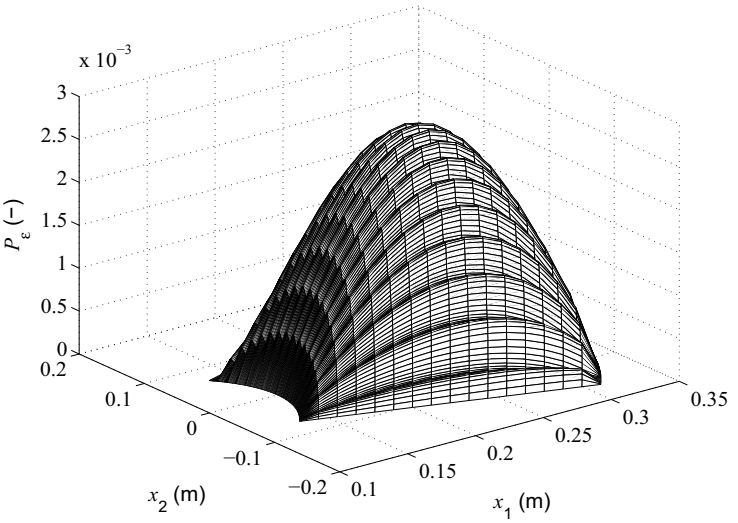

Figure 4.2: The dimensionless pressure distribution, P_ε, $\varepsilon = 1/2^4$, due to the surface roughness described by (4.54) at an intermediate time step t_k.

Figure 4.3 represents a plot of

$$\int_\Omega \left| P^{\pm}(x, \tau_k) - P_0(x, \tau_k) \right| \, dx / \int_\Omega P^{\pm}(x, \tau_k) \, dx,$$

(i.e. the relative difference between the solutions) against the discrete τ step (τ_k) for an eight step full overtaking cycle. In this simulation a single period of the sinusoids were discretely represented by 64 spatial nodes and this lead to a maximum relative difference.

The deterministic load carrying capacity $l_\varepsilon(t_k) = \int_\Omega P_\varepsilon(x, t_k) \, dx$ and the load carrying capacity $l_0(\tau_k) = \int_\Omega P_0(x, \tau_k) \, dx$ associated with the homogenized solution is depicted in Figure 4.4.

It is observed that for $\varepsilon = 1/2^6$ the difference between the load carrying capacities associated with the deterministic solution p_ε and the homogenized solution p_0 is small. In fact it attains a maximum value which is less than 2.5%, half way through the overtaking cycle (i.e. at time τ_k for $k = 4$).

In Figure 4.5 the pressure solution $P_\varepsilon(x_1, R_m, t_7)$, where $R_m = (R_1 + R_2)/2$ for three different choices of $\varepsilon = 1/2^4, 1/2^5$ and $1/2^6$ are shown, whilst Figure 4.6, depicts the area within the bearing, where the maximum pressures of the deterministic solutions and that of the of the homogenized solution (dashed line) may be observed. For clarity, an enlarged portion of the inlet

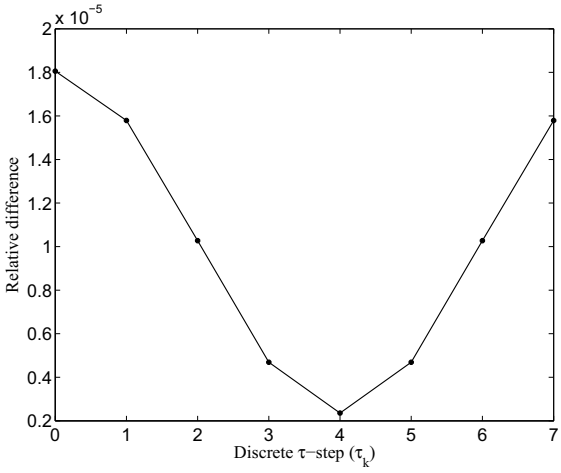

Figure 4.3: The relative difference between the aritmetic-harmonic bounds- and the homogenized- solution in terms of load carrying capacity as functions of τ.

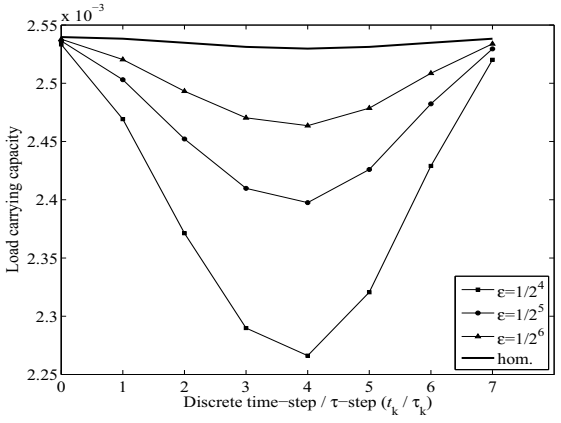

Figure 4.4: The deterministic-, for three choices of ε, and the homogenized-load carrying capacity in τ. Film thickness given by (4.54).

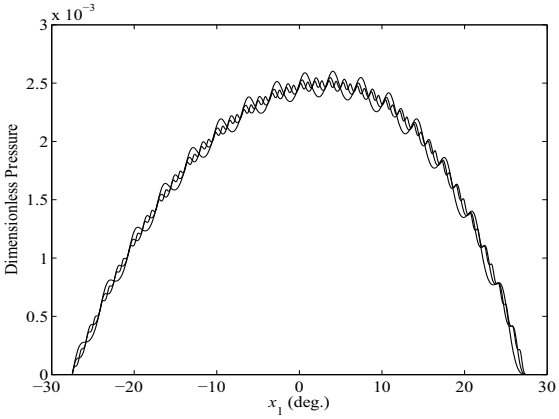

Figure 4.5: The pressure solution at $x_2 = R_m$, for three different choices of ε.

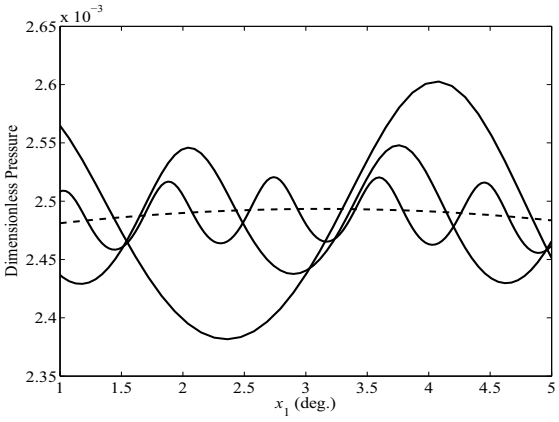

Figure 4.6: An enlarged portion showing the maximum pressure zone of the pressure solutions found in Figure 4.5 that also includes the homogenized solution (dashed line).

zone from Figure 4.5 is displayed in Figure 4.7.

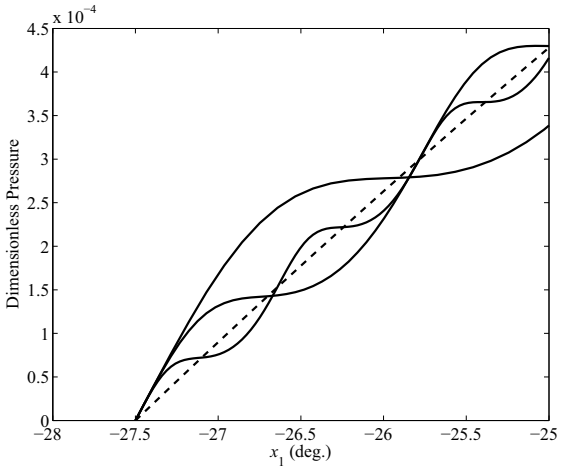

Figure 4.7: An enlarged portion showing the inlet zone of the pressure solutions found in Figure 4.5 that also includes the homogenized solution (dashed line).

Figure 4.8 is a display of an enlarged portion of the determinstic pressure solution P_ε, for $\varepsilon = 1/2^6$ and the homogenized solution P_0 at three different τ steps. In particular, this Figure illustrates the unstationary behavior of the Reynolds equation. Finally, the Reuss-Voigt bounds are compared to the homogenized solution. In Figure 4.9 the Reuss-Voigt bounds pressure solutions $P^{\pm}_{RV}$ and the homogenized solution P_0 are displayed at an intermediate τ step (τ_2) and Figure 4.10 visualizes the measure of the relative differences $\int_\Omega \left| P^{\pm}_{RV}(x,\tau_k) - P_0(x,\tau_k) \right| \, dx / \int_\Omega P_0(x,\tau_k) \, dx$, seen as functions of τ_k. From this figure it may be observed that the Reuss-Voigt bounds approximates the homogenized quite well, however, the maximum difference between the upper and the lower bound is approximately 5%.

4.4.3 Bisinusoidal roughness

Next we consider bisinusoidal surface roughness (i.e roughness in both directions) by defining H_{U} and H_{L} as

$$H_{\mathrm{U}}(y_1,\tau) = -\frac{c}{2}\left(\cos(2\pi y_1)\cos(2\pi y_2) - 1\right), \tag{4.55}$$
$$H_{\mathrm{L}}(y_1,\tau) = \frac{c}{2}\left(\cos\left(2\pi\left(y_1 - \omega_{\mathrm{L}}\tau\right)\right)\cos(2\pi y_2) - 1\right).$$

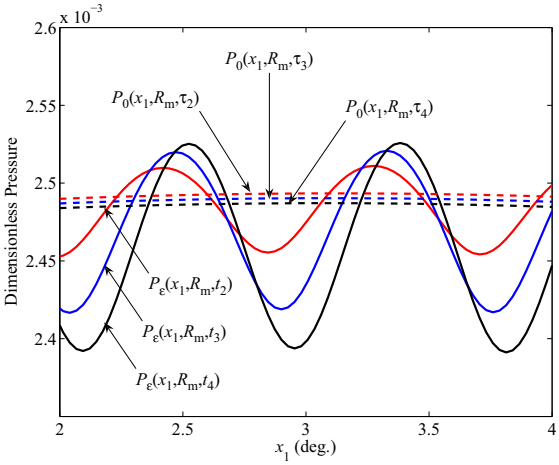

Figure 4.8: The determinstic pressure solution P_ε, for $\varepsilon = 1/2^6$ and the homogenized solution P_0 at three different τ steps.

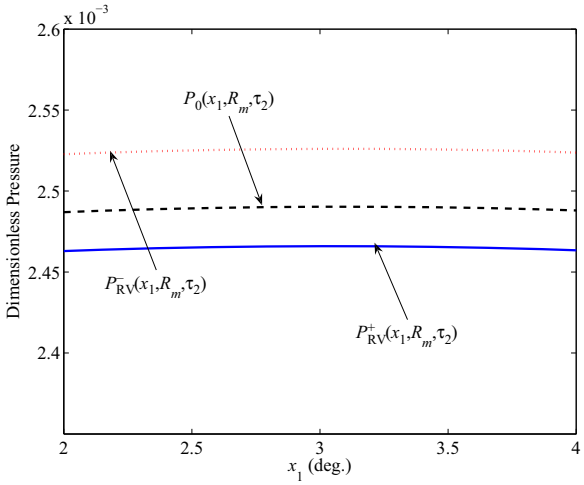

Figure 4.9: The Reuss-Voigt bounds pressure solutions $P^{\pm}_{RV}$ and the homogenized solution P_0 at an intermediate τ step.

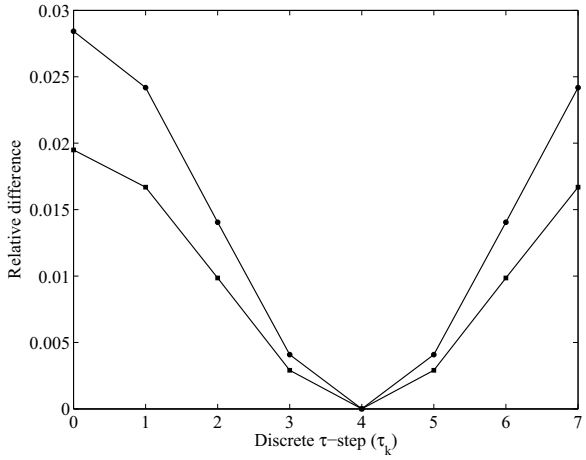

Figure 4.10: The relative difference between the Reuss-Voigt bounds solutions, upper bound ($^+$)- filled squares, lower bound ($^-$)- filled circles, and the homogenized- solution in terms of load carrying capacity as functions of τ

We again choose $c = 1/8$ and $\omega_{\mathrm{L}} = 100$ RPM $= 100\pi/30$ rad/s. The pressure distribution P_ε, $\varepsilon = 1/2^4$, is shown in Figure 4.11. The ε-convergence measured in terms of load carrying capacity (being a function of τ) is shown in Figure 4.12. We note that, each period of the deterministic, bisinusoidal, roughness representation is resolved with only 8 discrete grid nodes, meaning a total number of 513×513 grid nodes for $\varepsilon = 1/2^6$. In this case the arithmetic-harmonic bounds pressure solution is not equal to the homogenized one but Figure 4.13 reveals that the difference between the upper- and the lower- bound pressure solution is small, if measured in terms of load carrying capacity. In the case of bisinusoidal surface roughness, we also observe that the Reuss-Voigt bounds are close, with the difference between the upper and the lower bound almost as small as for the arithmetic-harmonic bounds, with the maximum difference being less than approximately 2.40% as compared to ($\approx 1.03 + 1.35 =$) 2.38% for the arithmetic-harmonic bounds .

4.4.4 A realistic surface roughness representation

In Figure 4.14, a surface originating from an optical interference measurement is shown. The ground original surface was coarsened by resampling

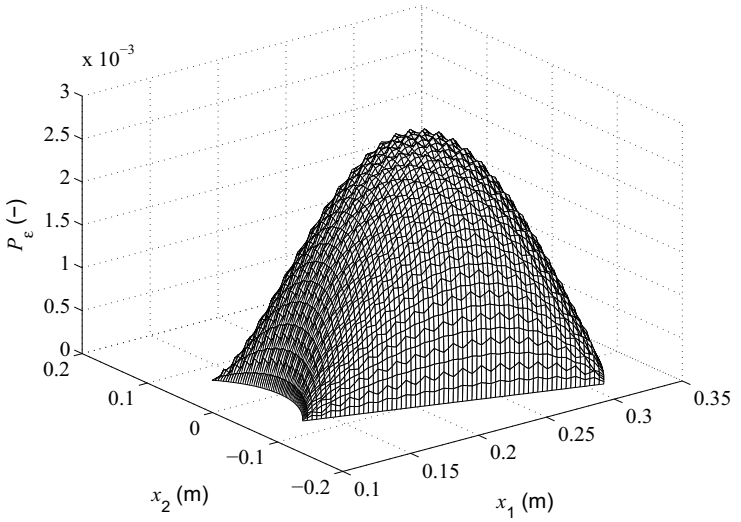

Figure 4.11: The dimensionless pressure distribution, P_ε, $\varepsilon = 1/2^4$, due to the surface roughness described by (4.55) at an intermediate time step t_k.

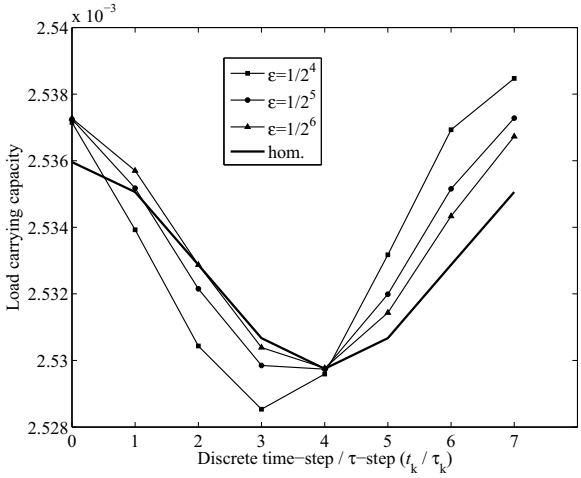

Figure 4.12: The deterministic-, for three choices of ε, and the homogenized-load carrying capacity in τ. Film thickness given by (4.54).

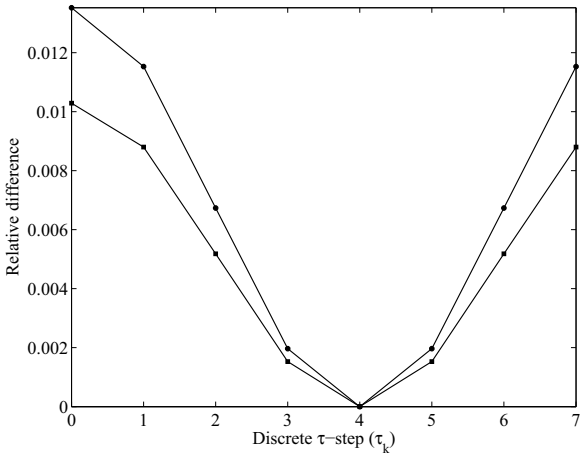

Figure 4.13: The relative difference between the arithmetic-harmonic bounds solutions, upper bound ($^+$)- filled squares, lower bound ($^-$)- filled circles, and the homogenized- solution in terms of load carrying capacity as functions of τ.

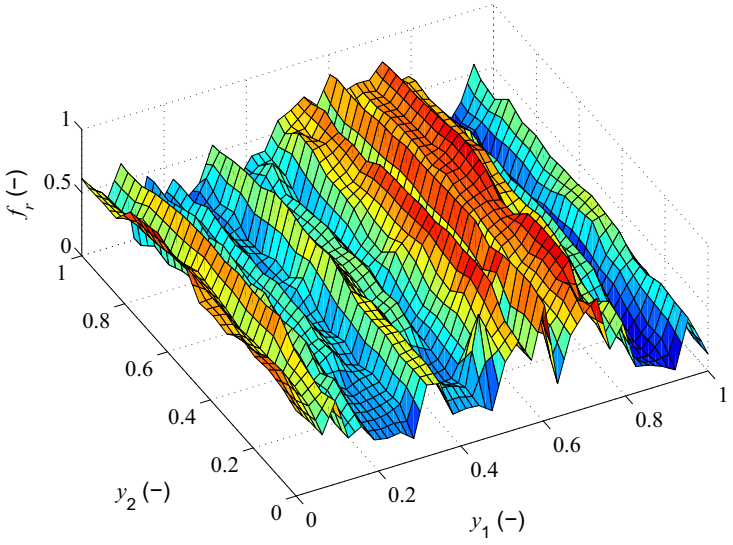

Figure 4.14: A surface roughness representation originating from a surface measurement.

on a 17×33 grid and then normalized. Note that the reason for coarsening, is to enable succesive linear interpolation in order to be able to reduce the discretization errors of the homogenized pressure solution to a tolerable level. For the results presented here, each period was interpolated onto 65×129 discrete nodes. Let us define this surface roughness representation function f_r, as the periodic extension of the measured specimen to the whole of $\mathbb{R}^2$. This makes it possible to state the dimensionless forms of surface roughness contribution to the the upper and the lower, in a way similar to what was done in the two previous model problems ($c = 1/8$ and $\omega_{\mathrm{L}} = 100$ RPM $= 100\pi/30$ rad/s), as

$$\begin{aligned} H_{\mathrm{U}}(y_1, \tau) &= -c\left(f(y_1, y_2) - 1\right), \\ H_{\mathrm{L}}(y_1, \tau) &= c\left(f(y_1 - \omega_{\mathrm{L}}\tau, y_2) - 1\right). \end{aligned} \tag{4.56}$$

Solving the deterministic problem for $\varepsilon = 1/2^3$, corresponding to the surface roughness representation (4.56) with f_r as in Figure 4.14, yields the pressure distribution at an intermediate time step t_k as shown in Figure 4.15. This

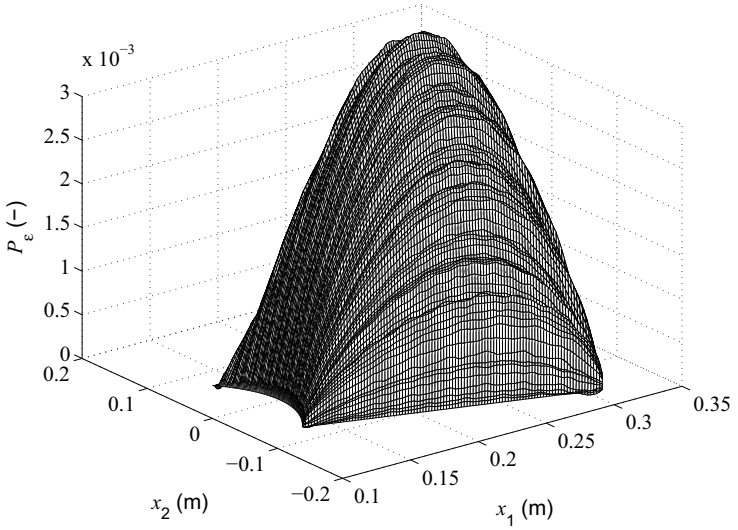

Figure 4.15: The dimensionless pressure distribution, P_ε, $\varepsilon = 1/2^3$, due to the surface roughness representation (4.56) with f_r as in Figure 4.14 at an intermediate time step t_k.

model problem, of course, causes much more trouble while being solved numerically, than the two having well defined mathematical surface roughness

descriptions that was previously considered. First of all the numerical error in the deterministic solution is greater, even though the problem was solved with 5 extra grid nodes ($17 \times 33 \longrightarrow 65 \times 129$ which is then repeated 8 times in each direction, meaning a solution domain consisting of 513×1025 grid nodes) linearly interpolated in between the points on the sampled surface. The homogenized solution is based on computations of local problems (4.19) and (4.20) represented on 65×129 and 129×257 grid nodes, i.e., 5 and 9 additional points linearly interpolated in between the sampled ones. Figure 4.16 displays the deterministic- and the homogenized- pressure solu-

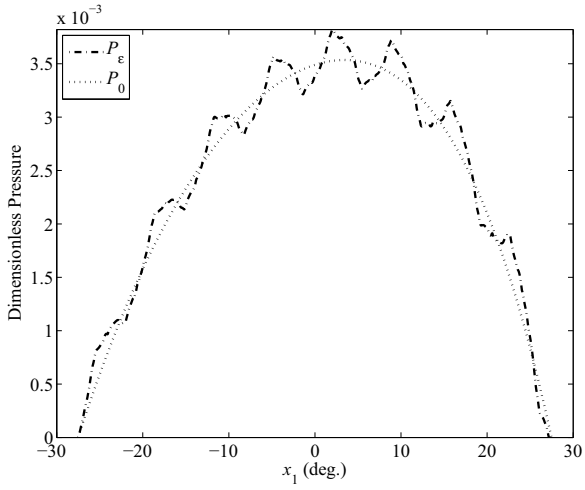

Figure 4.16: Display of the deterministic- and the homogenized- pressure solutions at $x_2 = R_m$ (at an intermediate τ-step).

tions at $x_2 = R_m$ (at an intermediate τ-step) and Figure 4.17, where both types of bounds pressure solutions have also been added, is an enlargement of the maximum pressure zone. It is evident from this Figure that the homogenized pressure solution, at R_m, is bounded by the arithmetic-harmonic pressure solutions, which also holds for the other model problems. However, the integrated absolute difference between the homogenized pressure obtained by solving the local problems at these two different resolutions, i.e., the discretization errors in the homogenized solution, is of the same magnitude, in fact less than 0.5%, as the difference between the upper and lower arithmetic-harmonic type bounds solutions. At another τ-step the homogenized pressure is not bounded by the bounds pressure solutions as shown in Figure 4.18.

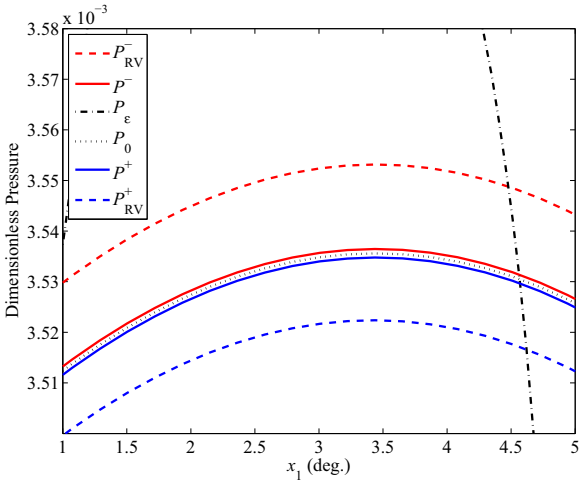

Figure 4.17: An enlarged portion showing the maximum pressure zone of the pressure solutions due to the surface roughness representation (4.56) with f_r as in Figure 4.14 at an intermediate τ-step τ_k.

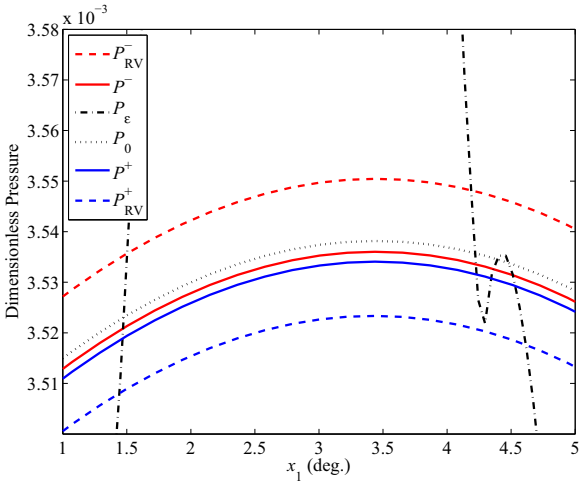

Figure 4.18: Similar to Figure 4.17 but at the following τ-step τ_{k+1}.

4.5 Concluding Remarks

The numerical results presented here confirms that homogenization is very useful in the analysis of hydrodynamically lubricated rough surface problems. In particular the recently introduced concept of bounds is shown to yield accurate estimates on the homogenized solution. A direct numerical computation of the homogenized pressure p_0 will require quite a lot of computational time since it involves solving cell problems. The bounds obtained make it possible to estimate p_0 at a significantly lower cost.

It has been demonstrated clearly, how the formal method of multiple scales expansion may be used to homogenize an unstationary problem formulated in terms of a variational principle. The homogenized results obtained by this method agrees with those obtained by Bayada et. al. in [10], where the method of two-scale convergence was used. The different types of bounds results obtained in this paper were based on the formulation of the Reynolds equation as a minimization problem.

It was proved in [8] that the arithmetic-harmonic type of bounds we have derived here, are sharp (or precise), in the sense that they coincide in the case of transversal or longitudinal surface roughness representations which is proved numerically by the model problem with sinusoidal roughness.

The model problem with bisinusoidal surface roughness representation shows that the Reuss-Voigt bounds pressure solutions may fairly well approximate the arithmetic-harmonic ones.

Finally, the numerical results from the more realistic model problem, having the surface roughness as depicted in Figure 4.14, shows even more precise bounds pressure solutions than for the previous problems. The numerical discretization error of the homogenized solution was even larger than the difference between the bounds for the case of a combined surface roughness amplitude ($2c$) being $1/4$ of the minimum film thickness of the corresponding smooth problem.

Bibliography

[1] G. Allaire. Homogenization and two scale convergence. *SIAM J. Math. Anal.*, 23(6):1482–1518, 1992.

[2] G. Allaire, A. Braides, G. Buttazzo, A. Defranceschi, and L.Gibiansky. School on Homogenization, ictp, Lect. notes, 4-17 september 1993. *Preprint SISSA, Trieste*, 1993.

[3] A. Almqvist. *On the Effects of surface Roughness in Lubrication.* PhD thesis, Department of Machine Elements, Luleå University of Technology, Sweden, 31, 2006.

[4] A. Almqvist and J. Dasht. The homogenization process of the Reynolds equation describing compressible liquid flow. *Tribol. Int.*, (39):994–1002, 2006.

[5] A. Almqvist, E. K. Essel, J. Fabricius, and P. Wall. Bounds for the unstationary incompressible Reynolds equation. Research report,(2007), Department of Mathematics, Luleå University of Technology, Sweden, submitted (17 pages).

[6] A. Almqvist, E. K. Essel, L.-E. Persson, and P. Wall. Homogenization of the unstationary incompressible Reynolds equation. *Tribol. Int. (in press), (18 pages)*, 2007.

[7] A. Almqvist, R. Larsson, and P. Wall. The Homogenization process of the time dependent Reynolds equation describing compressible liquid flow. Research report, No. 4, ISSN 1400-4003, Department of Mathematics, Luleå University of Technology, Sweden, 2006, submitted.

[8] A. Almqvist, D. Lukkassen, A. Meidell, and P. Wall. New concepts of homogenization applied in rough surface hydrodynamic lubrication. *To appear in Int. J. Eng. Sci.*, 2006.

[9] G. Bayada and M. Chambat. Homogenization of the Stokes system in a thin film flow with rapidly varying thickness. *Model. Math. Anal. Numer.*, 23(2):205–234, 1989.

[10] G. Bayada, S. Ciuperca, and M. Jai. Homogenization of variational equations and inequalities with small oscillating parameters. Application to the study of thin film unstationary lubrication flow. *C. R. Acad. Sci. Paris t. Serie*, 328:819–824, 2000.

[11] G. Bayada and J. B. Faure. A Double scale analysis approach of the Reynolds roughness comments and application to the journal bearing. *J. Tribol.*, 111:323–330, 1989.

[12] A. Bensoussan, J. L. Lions, and G. Papanicolaou. *Assymptotic Analysis for Periodic Structures*. North-Holland, Amsterdam, 1978.

[13] G. Buscaglia, I. Ciuperca, and M. Jai. Homogenization of the transient Reynolds equation. *Asymptot. Anal.*, 32:131–152, 2002.

[14] G. Buscaglia and M. Jai. Sensitivity analysis and Taylor expansions in numerical homogenization problems. *Numer. Math.*, 85:49–75, 2000.

[15] G. Buscaglia and M. Jai. A new numerical scheme for non uniform homogenized problems: Application to the non linear Reynolds compressible equation. *Math. Probl. Eng.*, 7(4), 2001.

[16] G. Buscaglia and M. Jai. Homogenization of the generalized Reynolds equation for ultra-thin gas films and its resolution by fem. *J. Tribol.*, 126:547–552, 2004.

[17] D. Cioranescu and P. Donato. *An introduction to homogenization*. Oxford University Press, New York, 1999.

[18] H. G. Elrod. A cavitation algorithm. *J. Lubr. Technol.*, 103:350–354, 1981.

[19] M. Jai. Homogenization and two-scale convergence of the compressible Reynolds lubrication equation modelling the flying characteristics of a rough magnetic head over a rough rigid-disk surface. *RAIRO Modél. Math. Anal. Numér.*, 29(2):199–233, 1995.

[20] M. Jai and B. Bou-Said. A comparison of homogenization and averaging techniques for the treatment of roughness in slip-flow-modified Reynolds equation. *J. Tribol.*, 124:327–335, 2002.

[21] V. V. Jikov, S. M. Kozlov, and O. A. Oleinik. *Homogenization of Differential Operators and Integral Functionals*. Springer- Verlag, Berlin-Heidelberg-New York, 1994.

[22] M. Kane and B. Bou-Said. Comparison of homogenization and direct techniques for the treatment of roughness in incompressible lubrication. *J. Tribol.*, 126:733–737, 2004.

[23] M. Kane and B. Bou-Said. A study of roughness and non-newtonian effects in lubricated contacts. *J. Tribol.*, 127:575–581, 2005.

[24] J. L. Lions, D. Lukkassen, L.-E Persson, and P. Wall. Reiterated homogenization of nonlinear monotone operators. *Chinese Ann. Math. Ser. B*, 22:1–12, 2001.

[25] D. Lukkassen, A. Meidell, and P. Wall. Bounds on the effective behaviour of a homogenized reynolds-type equation. Research report,No. 3, ISSN 1400-4003, Department of Mathematics, Luleå University of Technology, Sweden, 2006.

[26] G. Nguetseng, D. Lukkassen, and P. Wall. Two-scale convergence. *Int. J. Pure Appl. Math.*, 2(1):35–86, 2002.

[27] L. E. Persson, L. Persson, N. Svanstedt, and J. Wyller. *The homogenization method: An introduction*. Studentlitteratur, Lund, 1993.

[28] P. Wall. Homogenization of Reynolds equation by two-scale convergence. Research report, No. 3, ISSN 1400-4003, Department of Mathematics, Luleå University of Technology, Sweden, 2005, to appear in Chinese Ann. Math.